

Bioorthogonal reaction

Staudinger ligation
&
Cu-free click chemistry

2013.11.18 Hanada (M1)

What are the requirements for reactions in living animals?

- Stability and reactivity under physiological conditions (water, pH, temperature)
- Selectivity and bioinertness (Lys, Cys, Tyr, etc. are included in cells)
- Low toxicity
- Rapid kinetics in low concentration

The concept of

1. Introduction

“Bioorthogonal reaction”

Central to the process of chemical cell-surface remodelling is the concept of bio-orthogonality. The pair of functional groups chosen for the cell-surface transformation must be mutually reactive under physiological conditions and, at the same time, remain inert to the biological environment.

Prescher, J. A.; Dube, D. H., Bertozzi, C. R. *Nature* **2004**, *430*, 873.



Prof. Carolyn Bertozzi is the T.Z. and Irmgard Chu Distinguished Professor of Chemistry and Professor of Molecular and Cell Biology at UC Berkeley, and Professor of Molecular and Cellular Biology at UCSF. She is also the Director of the Molecular Foundry at the Lawrence Berkeley National Laboratory and an Investigator of the Howard Hughes Medical Institute. She earned her AB in Chemistry from Harvard University in 1988 and obtained her PhD at UC Berkeley in 1993 with Prof. Mark Bednarski. She carried out postdoctoral research at UCSF with Prof. Steven Rosen and joined the faculty at UC Berkeley in 1996.

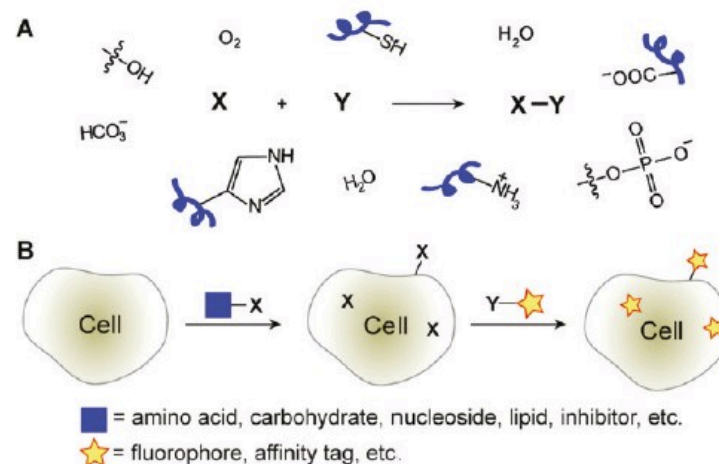


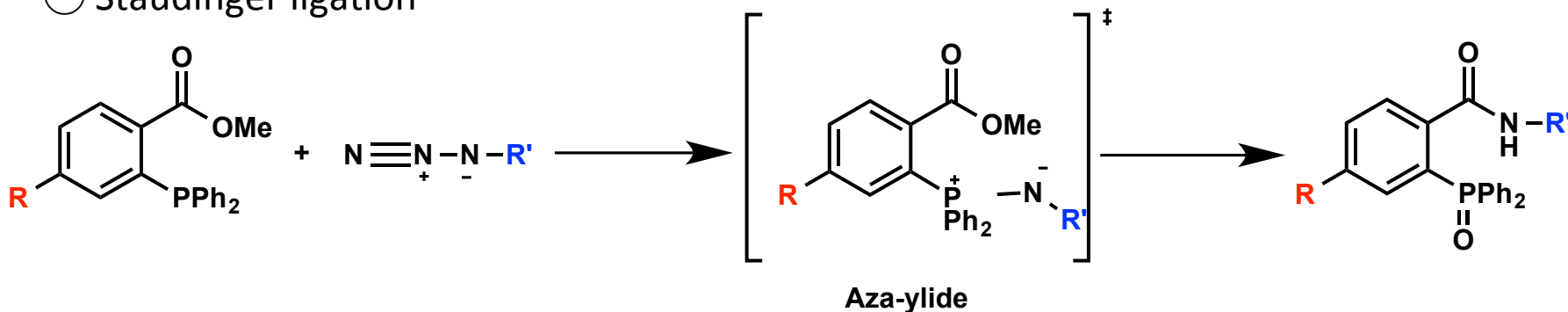
FIGURE 1. (A) A generic bioorthogonal chemical reaction between X and Y that proceeds in biological systems. (B) A common experimental platform for biomolecule probing using bioorthogonal chemistry. First, a non-native functional group, often called a “chemical reporter”, is installed in a biomolecule of interest. The modified biomolecule is subsequently labeled using a bioorthogonal chemical reaction.

Sletten, E. M.; Bertozzi, C. R. *Acc. Chem. Res.* **2011**, *44*, 666.

Sletten, E. M.; Bertozzi, C. R. *Angew. Chem. Int. Ed.* **2009**, *48*, 6974.

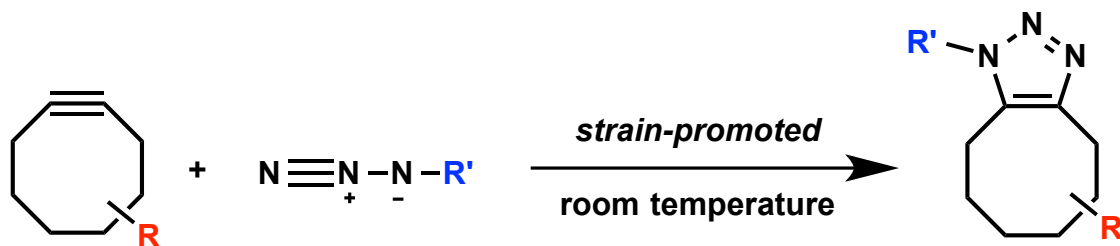
Today's contents

○ Staudinger ligation



Saxon, E. M. Bertozzi, C. R. *Science*. **2000**, 287, 2007.

○ Cu-free click chemistry



Agard, N. J. ; Prescher, J. A. ; Bertozzi, C. R. *J. Am. Chem. Soc.* **2004**, 126, 15046.

Index

1. Introduction
2. Staudinger ligation
 - 2-1. Basic development
 - 2-2. Cell surface investigation
 - 2-3. *Ex vivo* and *in vivo*
 - 2-4. Kinetics studies
3. Cu-free click chemistry
 - 3-1. Precedents and prototype reactions
 - 3-2. Strain promoted [3+2] cycloaddition
 - 3-3. DIFO/BARAC
 - 3-4. Advanced labeling with DIFO *in vivo*
4. Summary

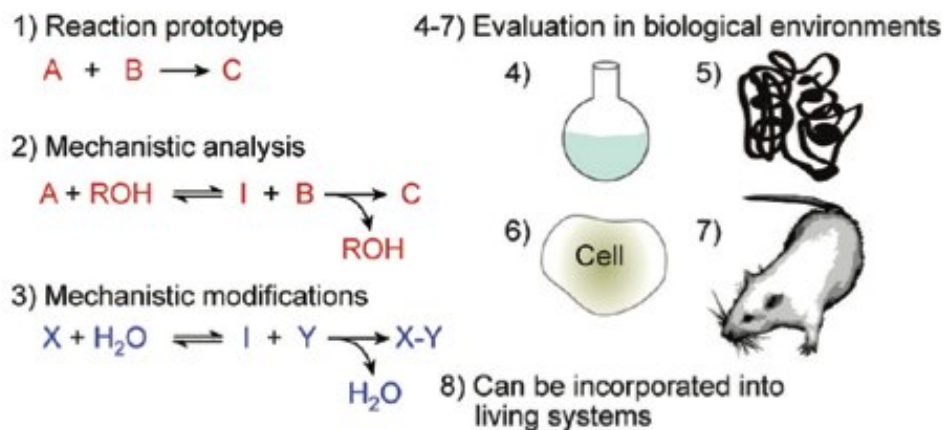
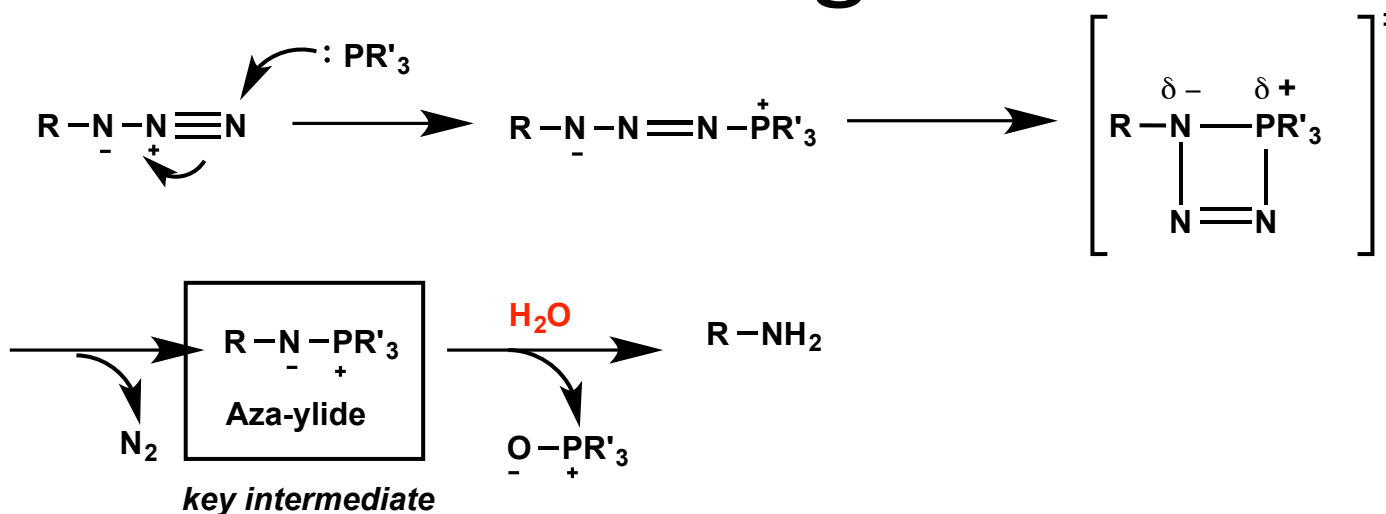


FIGURE 3. A step-by-step guide to developing a bioorthogonal reaction.

Classical Staudinger reaction



○ Physiological condition & Bioinertness

- The phosphine and azide forms Aza-ylide in the presence of water at RT.
- Both are abiotic and expected to be bioinert.

Points to overcome

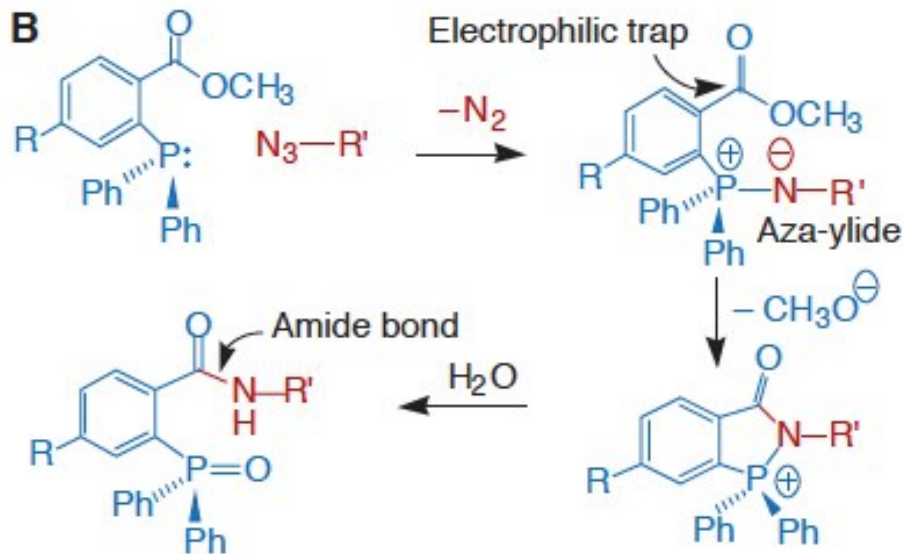
× Aza-ylide intermediate hydrolyzes to yield amine.

△ water solubility of Phosphine

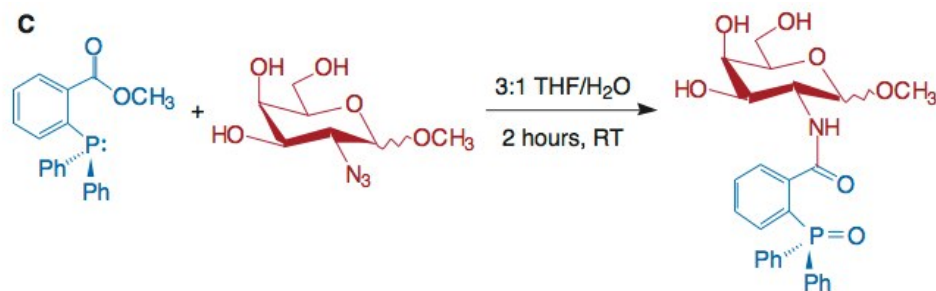
Sletten, E. M. Bertozzi, C. R. *Acc. Chem. Res.* **2011**, *44*, 666.

Molecular design through small molecule investigation

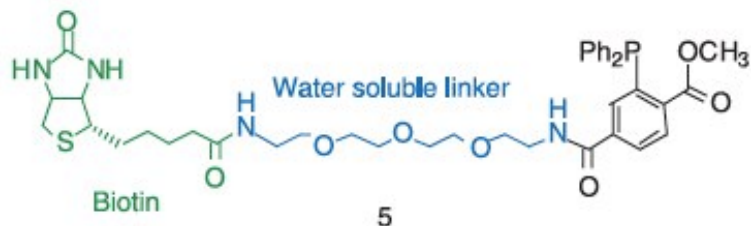
- Intramolecular reaction was designed in order to prevent amine formation.



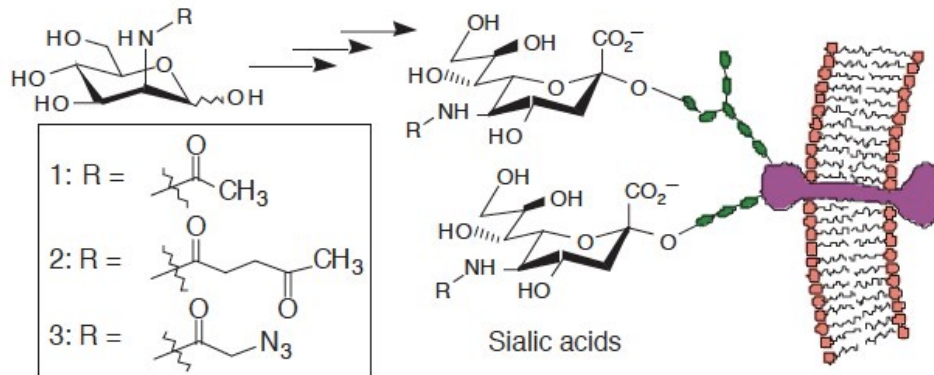
- The model reaction gave only a ligation product. (A primary amine was not observed.)



- Phosphine solubility was improved with water soluble linker.



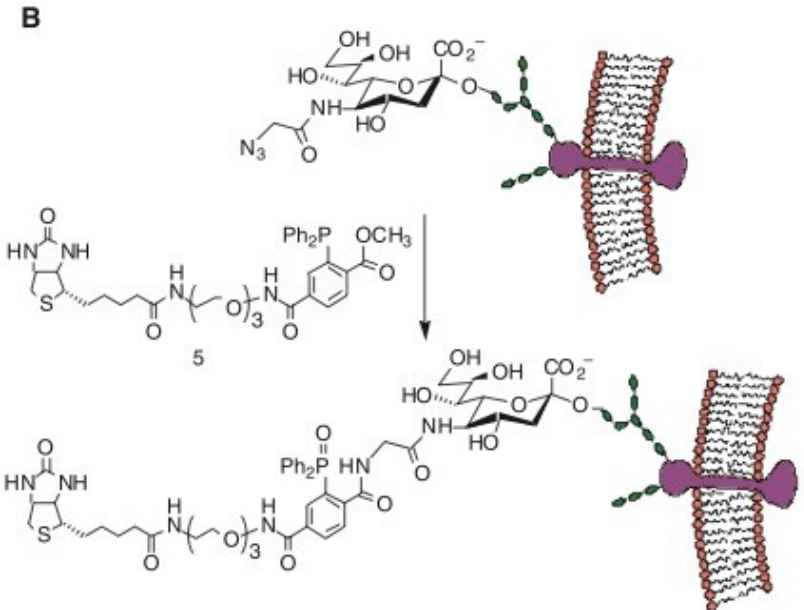
Reaction on the cell surface



1. Azide install via metabolic pathway

3. Detection

- Avidin- FITC fluorescence (Flow cytometry)
- HRP-conjugated biotin antibody (Western blotting)
- ...etc.



2. Staudinger ligation on the cell surface

Azide install Mechanism

- Modified ManNAc derivative was accepted in the biosynthetic pathway of the Sialoside.

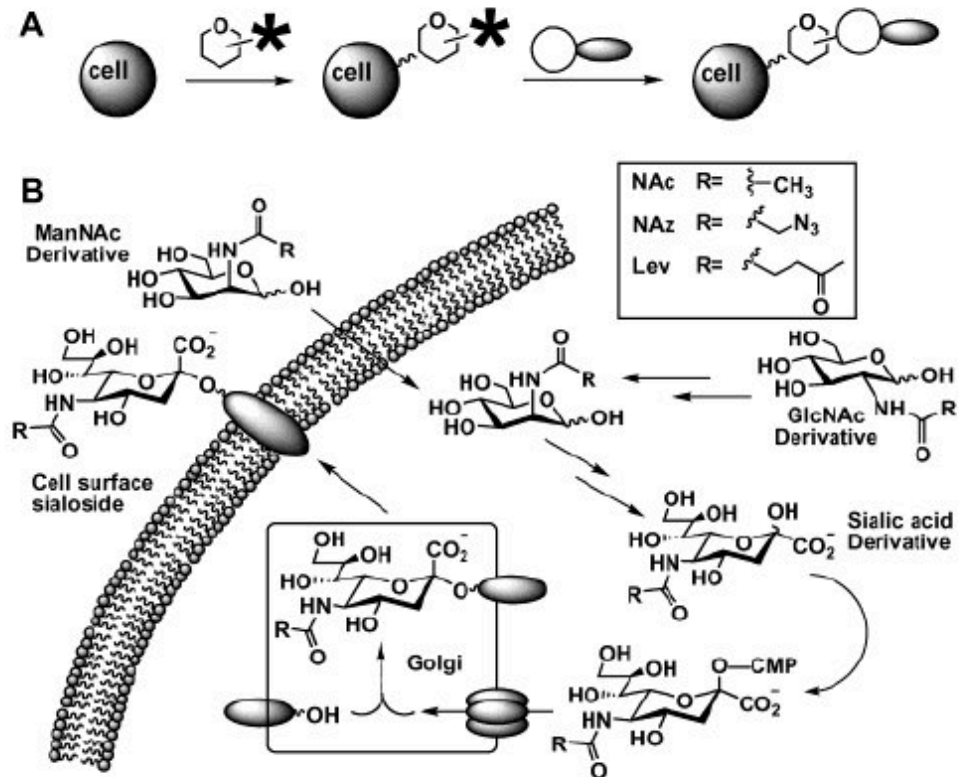


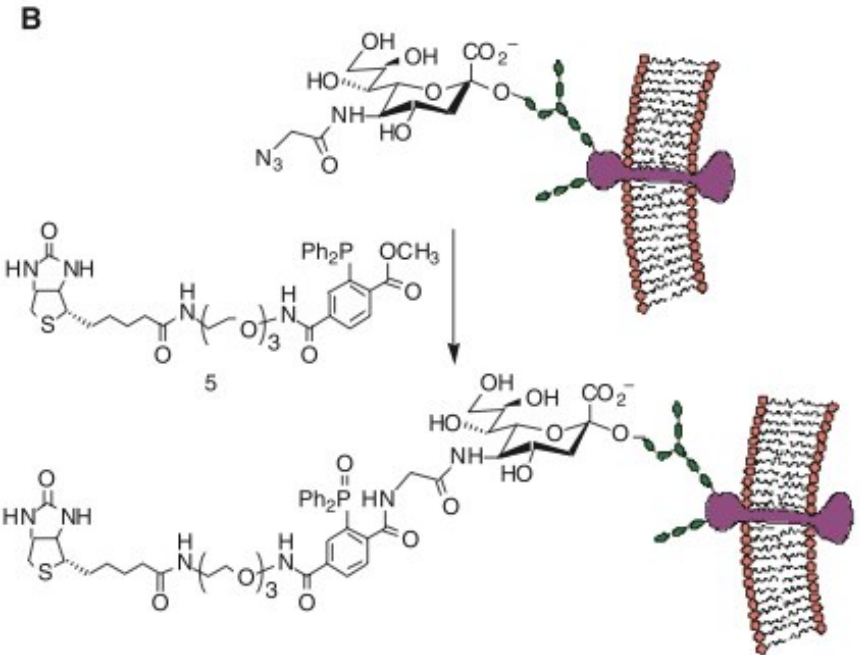
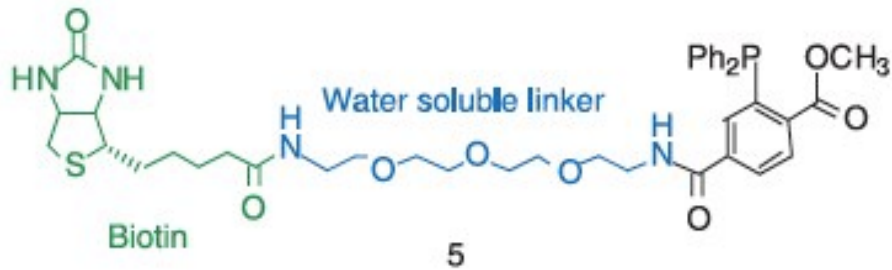
Figure 1. (A) Metabolism of a sugar bearing a selectively reactive functional group (*) results in its cell-surface display. Chemoselective ligation with an exogenously delivered reaction partner further modifies the cell-surface glycan. (B) Sialic acid biosynthetic pathway. Cell-surface sialosides are biosynthesized in a series of enzymatic steps. The process normally begins with either ManNAc or GlcNAc; however, exogenously added unnatural analogues of these compounds (or more advanced intermediates) are able to intercept the pathway and produce cell-surface sialosides with novel functionality.

Saxon, E. ; Bertozzi, C. R. *et al. J. Am Chem. Soc.* **2002**, *124*, 14893.

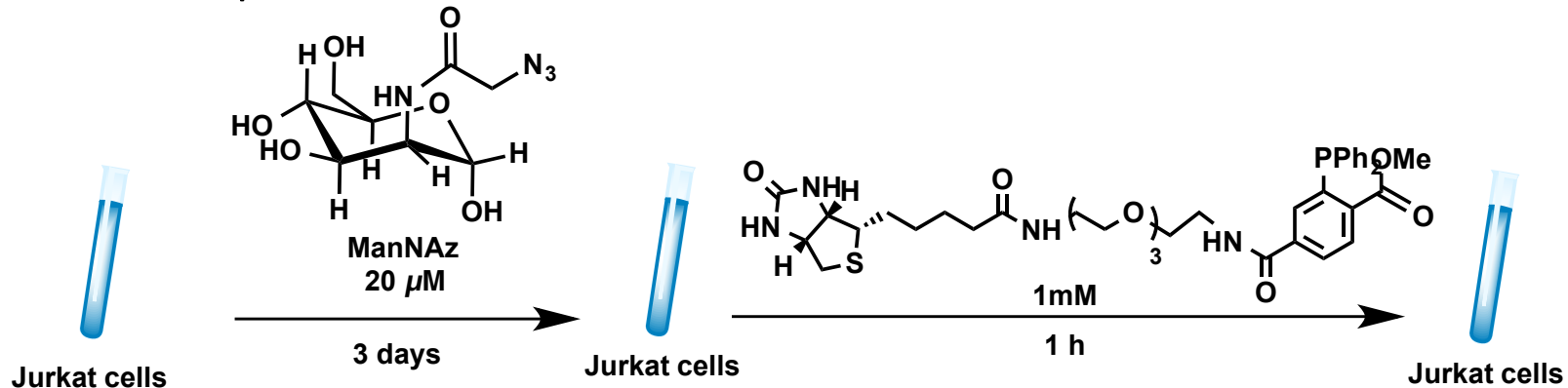
Yarema, K. J. ; Bertozzi, C. R. *et al. J. biol. Chem.* **1998**, *273*, 31168.

Ligation step

- Water soluble phosphin reagent

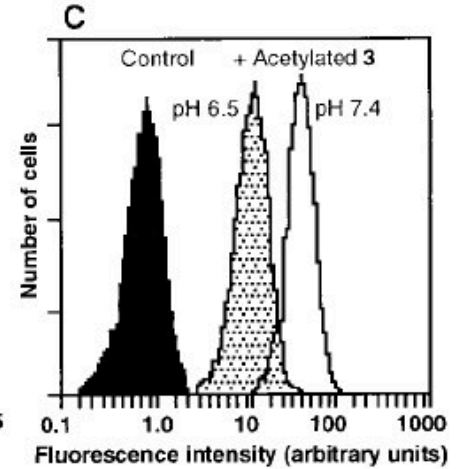
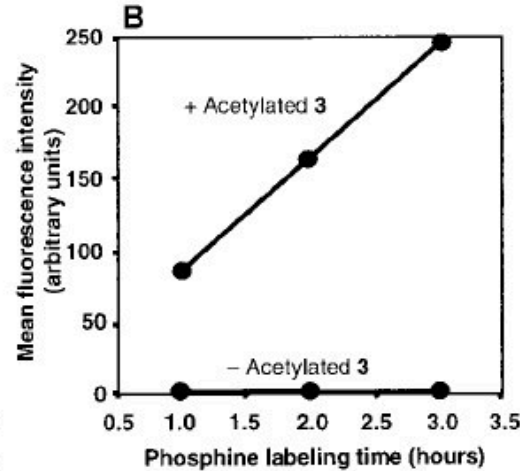
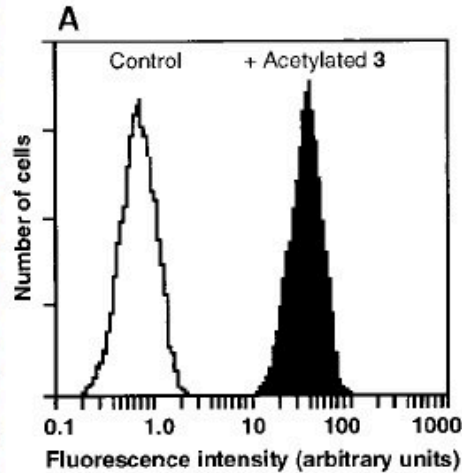


- Reaction procedure



Detection step

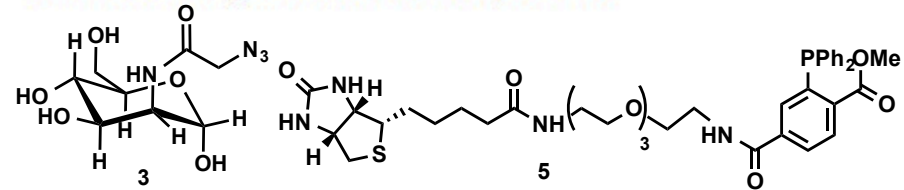
Fig. 4. (A) Analysis of cell surface reaction by flow cytometry. Jurkat cells (1.25×10^5 cells per milliliter) were cultured in the presence or absence (control) of acetylated **3** ($20 \mu\text{M}$ for 3 days). The cells were washed twice with 1 ml of buffer (0.1% fetal bovine serum in PBS, pH 7.4) and diluted to a volume of $240 \mu\text{l}$. Samples were added to $60 \mu\text{l}$ of a solution of **5** (5 mM in PBS, pH 7.4) and incubated at room temperature for 1 hour. The cells were washed and re-suspended in $100 \mu\text{l}$ of buffer, then added to $100 \mu\text{l}$ of FITC-avidin staining solution (1:250 dilution in PBS). After a 10-min incubation in the dark at 4°C , the cells were washed with 1 ml of buffer and the FITC-avidin staining was repeated. The cells were washed twice with buffer, then diluted to a volume of $300 \mu\text{l}$ for flow cytometry analysis. Similar results were



obtained in two replicate experiments. **(B)** Progress of reaction over time. Assays were performed as in **(A)** with $40 \mu\text{M}$ acetylated **3** and varying the duration of the reaction with compound **5**. **(C)** pH profile of reaction. Assays were performed as in **(A)** with $40 \mu\text{M}$ acetylated **3** and varying the pH of the buffer used during incubation with compound **5**.

- Cell surface labeling was detected by flow cytometry.

- Jurkat cells were stained with Avidin-FITC, and then detected by flow cytometry.

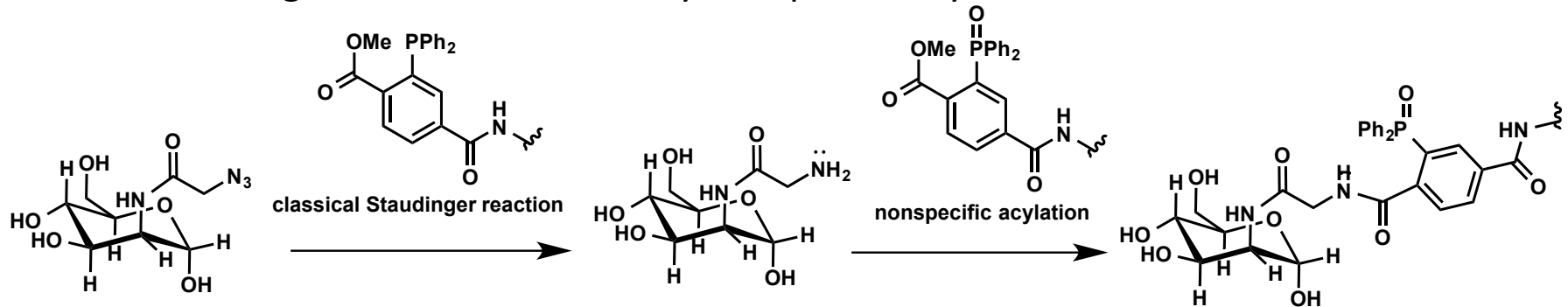


- Stained with Avidin-FITC, Jurkat cells which were treated with ManNAz and aryl phosphine showed high fluorescence.

→ But, is the reaction hypothesis really true?

Possible side reactions

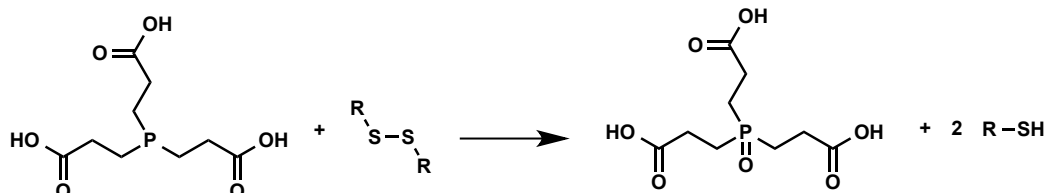
- Classical Staudinger reaction followed by nonspecific acylation of amines



- Reduction of disulfide bonds

Alkyl phosphine reduces disulfide bonds to thiol.

→ How about aryl phosphines?



TCEP

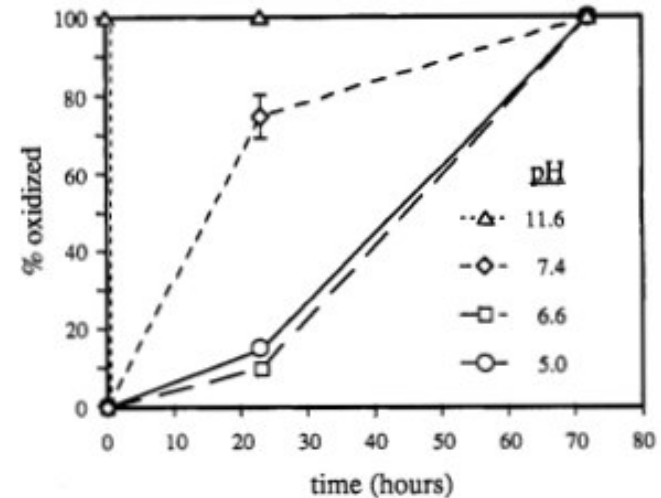


Figure 1. Solutions of TCEP (5 mM) in acetate or phosphate buffers (0.4 M) autoxidized slowly at pH <7. The solutions were stirred vigorously under air at room temperature and analyzed periodically by ^1H NMR spectroscopy.

Whitesides, G. M. *et al. J. Org. Chem.* **1991**, *56*, 2648.

Control experiments

It is confirmed that this fluorescence was not generated by reduction of disulfide bonds or non-specific acylation of amines.

→ *This reaction is a genuine bioorthogonal reaction!*

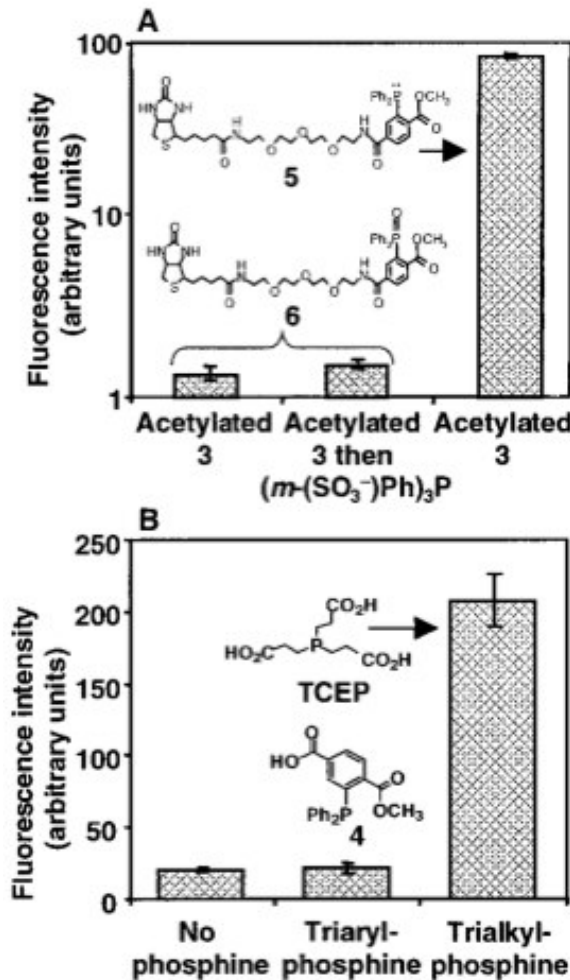


Fig. 5. Specificity of the modified Staudinger reaction. **(A)** Cell surface biotinylation does not proceed by classical Staudinger azide reduction followed by nonspecific acylation. Jurkat cells were cultured in the presence of acetylated **3** as described in Fig. 4. Cell surface azides were either reduced intentionally with a trisulfonated triphenylphosphine or left unreduced. Phosphine oxide **6**, the product of the classical Staudinger reaction, was prepared independently and incubated with the cells (1 mM for 1 hour). Analysis by flow cytometry was performed as in Fig. 4. **(B)** Triarylphosphines do not reduce disulfide bonds at the cell surface. Jurkat cells were incubated with a 1 mM solution of triarylphosphine **4** or TCEP for 1 hour at room temperature. The cells were centrifuged (2 min, 3000 g), washed with PBS, and diluted to a volume of 240 μ l. Samples were combined with 60 μ l of a solution of iodoacetylbiotin (5 mM in PBS). After incubation in the dark at room temperature for 1.5 hours, the cells were washed with buffer, stained with FITC-avidin, and analyzed by flow cytometry. In both **(A)** and **(B)**, error bars represent the standard deviation of two replicate experiments.

Ex vivo (Ac₄ManNAz metabolization *in vivo*)

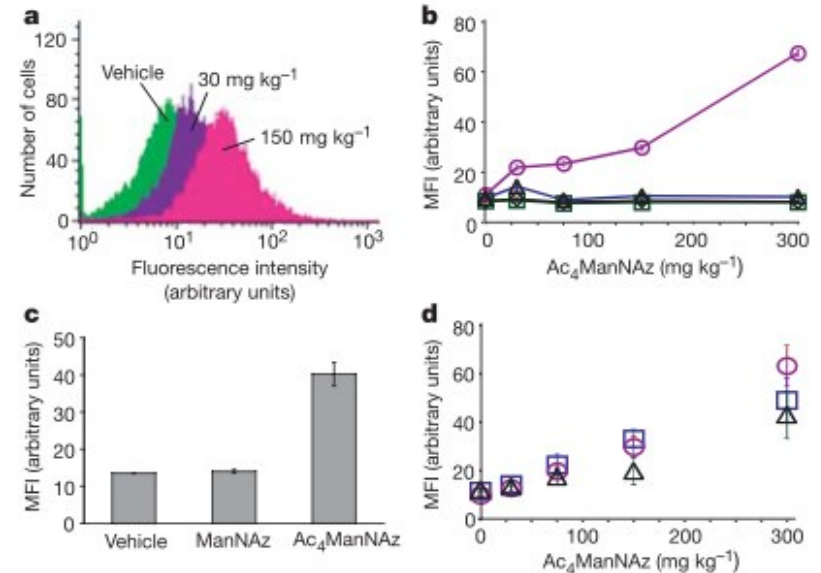
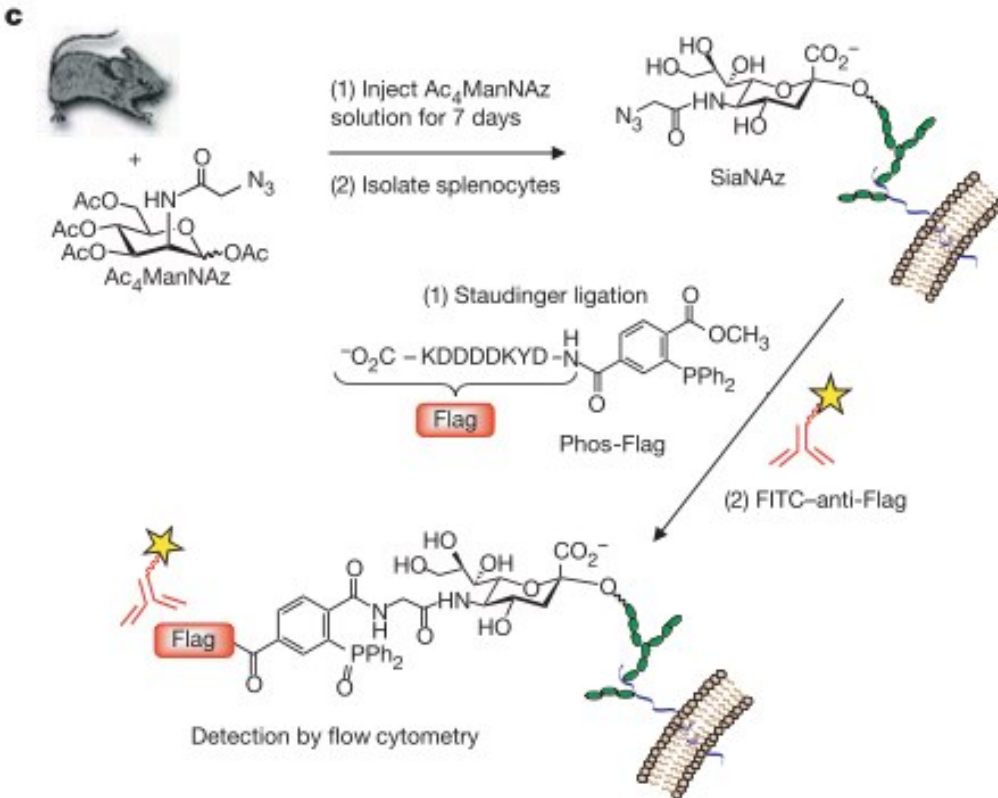
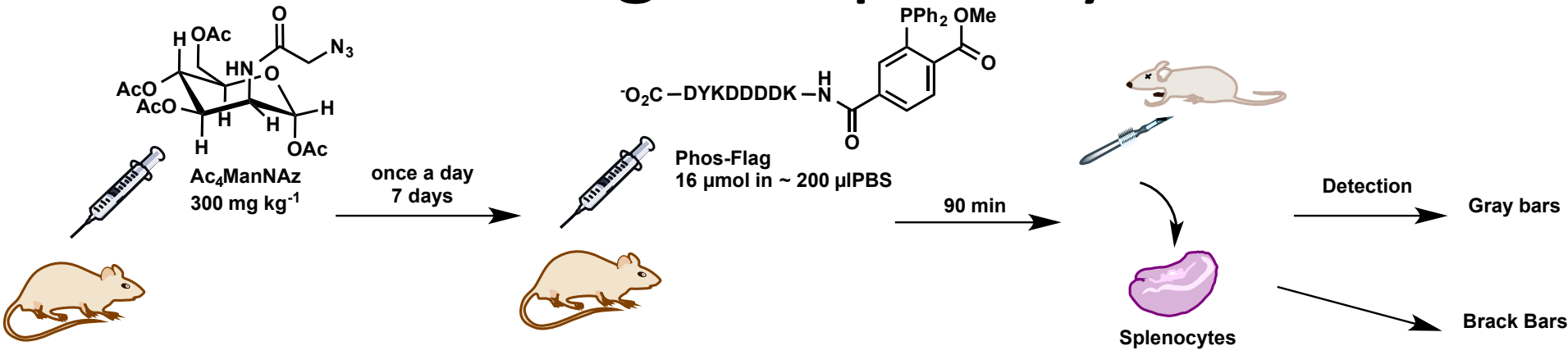


Figure 2 Ac₄ManNAz is metabolized *in vivo*. **a**, Flow cytometry analysis of splenocytes from Ac₄ManNAz-treated mice. **b**, Mean fluorescence intensity (MFI) of the cells from **a** as a function of azido-sugar dose (circles). Assay controls included unlabelled splenocytes from Ac₄ManNAz-treated mice (squares), splenocytes from Ac₄ManNAz-treated mice incubated with Phos-Flag followed by a class-matched control monoclonal antibody (diamonds), and splenocytes from Ac₄ManNAz-treated mice incubated with FITC-anti-Flag only (triangles). **c**, MFI of splenocytes from Ac₄ManNAz- and ManNAz-treated Es1^o/Es1^o mice. **d**, MFI of splenocytes from Es1^o/Es1^o mice (triangles) or wild-type B6D2F1 mice (circles, males; squares, females) treated with Ac₄ManNAz. Error bars represent the standard deviation of the mean for three replicate Staudinger ligation reactions. For **a-d** similar results were obtained in two replicate experiments.

• Ac₄ManNAz metabolization *in vivo* (mice) and Staudinger ligation *ex vivo* was demonstrated.

Cell labeling completely *in vivo*



▪ Staudinger ligation was successfully achieved *in vivo*.

But, some problemes still remained....

- Gradual phosphine air oxidation and metabolized by P-450
- High concentrations of phosphine occurred high background signal. (Washing away is difficult.)

Next : kinetics investigation in order to reduce the concentration of phosphine

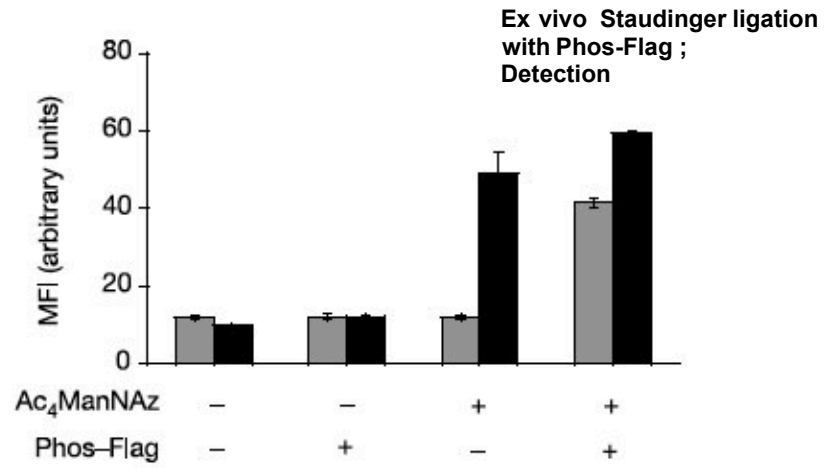
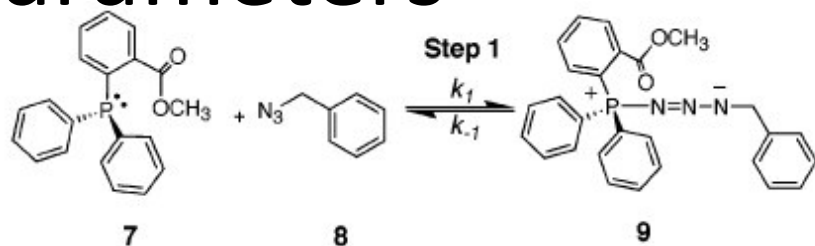


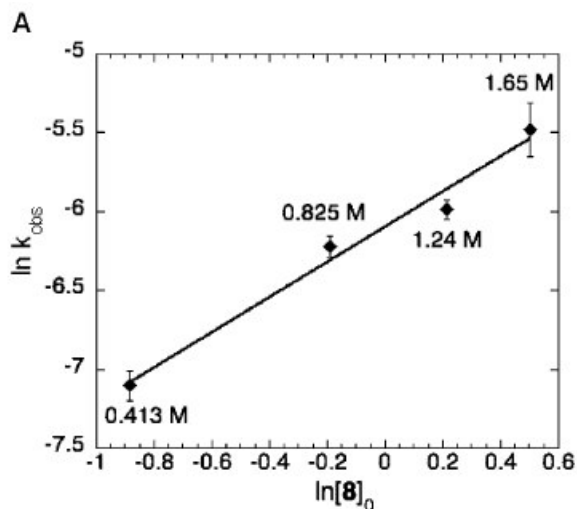
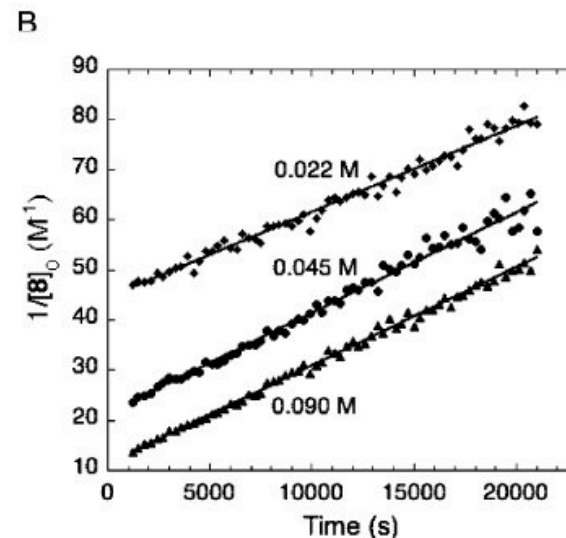
Figure 4 The Staudinger ligation proceeds *in vivo*. Mice were administered Ac_4ManNAz or vehicle once daily for 7 days. On the eighth day, the mice were administered Phos-Flag ($16 \mu\text{mol}$ in $\sim 200 \mu\text{l PBS}$) or an equal volume of vehicle. After 1.5 h, splenocytes were treated with FITC-anti-Flag and analysed by flow cytometry (grey bars). A portion of the isolated splenocytes was further reacted with Phos-Flag and analysed as in Fig. 2 (black bars). Error bars represent the standard deviation of the mean for three replicate FITC-anti-Flag labelling reactions or Staudinger ligation reactions.

Determination of the kinetic parameters



- The first step is presumed to be the rate-determining step.
- No intermediate was observed in ^{31}P NMR analysis.
- Measurement of pseudo-first order kinetics (k_{obs}) by ^{31}P NMR of **7** and **8** (1 : 10) in CD_3CN with 5% water (v / v)

- Analysis under the stoichiometric condition



$$[\mathbf{8}] \gg [\mathbf{7}]$$

$$v = k[\mathbf{7}][\mathbf{8}] \doteq k_{\text{obs}} [\mathbf{7}]$$

$$k_{\text{obs}} = k [\mathbf{8}]$$

$$\therefore \ln k_{\text{obs}} = \ln [\mathbf{8}] + \ln k$$

$$\ln [\mathbf{7}] = k_{\text{obs}} t + C$$

$$k = 2 \times 10^{-3} \text{ M}^{-1} \text{ s}^{-1}$$

Figure 1. Kinetic analysis of the Staudinger ligation of phosphine **7** and benzyl azide (**8**). (A) Plot of $\ln k_{\text{obs}}$ versus $\ln [\mathbf{8}]_0$ to determine the second-order rate constant under pseudo-first-order conditions, where **8** was used in excess. Pseudo-first-order rate constants were measured at $[\mathbf{7}] = 0.041 \text{ M}$ and $[\text{H}_2\text{O}] = 2.8 \text{ M}$ in CD_3CN at 20–21 °C. The second-order rate constant is calculated to be $(2.5 \pm 0.2) \times 10^{-3} \text{ M}^{-1} \text{ s}^{-1}$ from the y-intercept of the least-squares fit, with an estimated 10% error. (B) Plot of $1/[\mathbf{8}]_0$ versus time to determine the second-order rate constant of the Staudinger ligation between phosphine **7** and benzyl azide (**8**) under stoichiometric conditions in CD_3CN with 5% (v/v) H_2O . The slopes of the linear fits represent the second-order rate constants according to the kinetic model for a second-order reaction. At each concentration of substrate, linear fits were obtained with similar slopes of approximately $2 \times 10^{-3} \text{ M}^{-1} \text{ s}^{-1}$.

Phosphine substituents effects

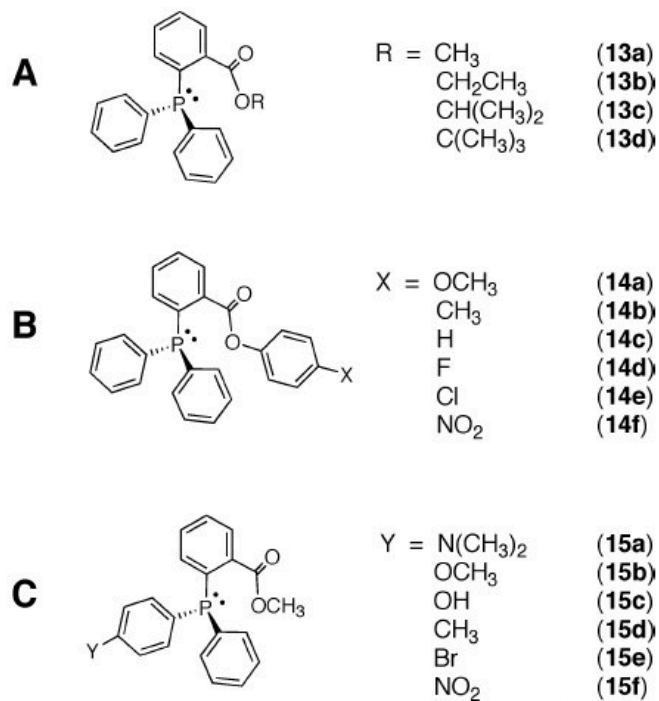


Figure 2. Phosphines synthesized to investigate the effects of steric and electronic modifications on the rate of the Staudinger ligation.

Table 2. Pseudo-First-Order Rate Constants and Product Distribution for the Staudinger Ligation of Phosphines **13a–d** and Benzyl Azide in CD₃CN with 5% (v/v) H₂O^a

phosphine	R	LP:HP ^b	k _{obs} (10 ⁻³ M ⁻¹ s ⁻¹)
13a	CH ₃	100:0	2.0 ± 0.1
13b	CH ₂ CH ₃	100:0	1.9 ± 0.1
13c	CH(CH ₃) ₂	100:0	2.0 ± 0.2
13d	C(CH ₃) ₃	60:40	1.8 ± 0.3

^a Reported rate constants represent the average of three runs under each condition ±5% standard deviation. ^b LP = ligation product; HP = hydrolysis product. Product ratios determined by ³¹P NMR peak integrations.

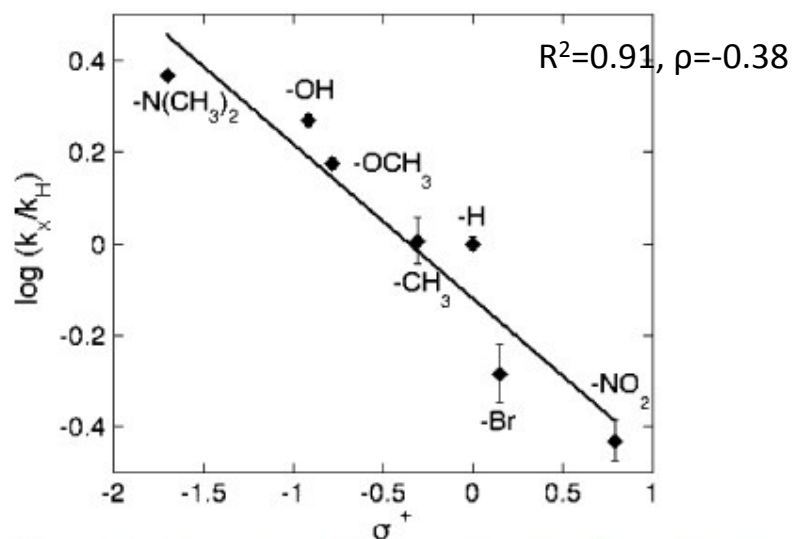


Figure 3. Hammett analysis for substituents on the phenyl group directly attached to the phosphorus center. Reactions were performed with phosphines **15a–f** (0.020 M) and benzyl azide (**8**) (0.83 M) in 5% (v/v) H₂O in CD₃CN at room temperature.

Table 3. Pseudo-First-Order Rate Constants of the Staudinger Ligation of Phosphines **14a–f** and Benzyl Azide in CD₃CN with 5% (v/v) H₂O^a

phosphine	X	σ_{para}^b	k _{obs} (10 ⁻³ M ⁻¹ s ⁻¹)
14a	OCH ₃	-0.27	2.0 ± 0.2
14b	CH ₃	-0.17	2.0 ± 0.2
14c	H	0	1.8 ± 0.2
14d	F	0.06	1.9 ± 0
14e	Cl	0.23	2.2 ± 0.1
14f	NO ₂	0.78	1.9 ± 0.4

^a Reported rate constants represent the average of three runs under each condition ±5% standard deviation. ^b Values are those given by Ritchie, C. D.; Sager, W. F. *Prog. Phys. Org. Chem.* **1964**, 2, 323.

Lin., F. L.; Bertozzi, C. R. *et al. J. Am. Chem. Soc.* **2005**, 127, 2687.

Phosphine modification effects

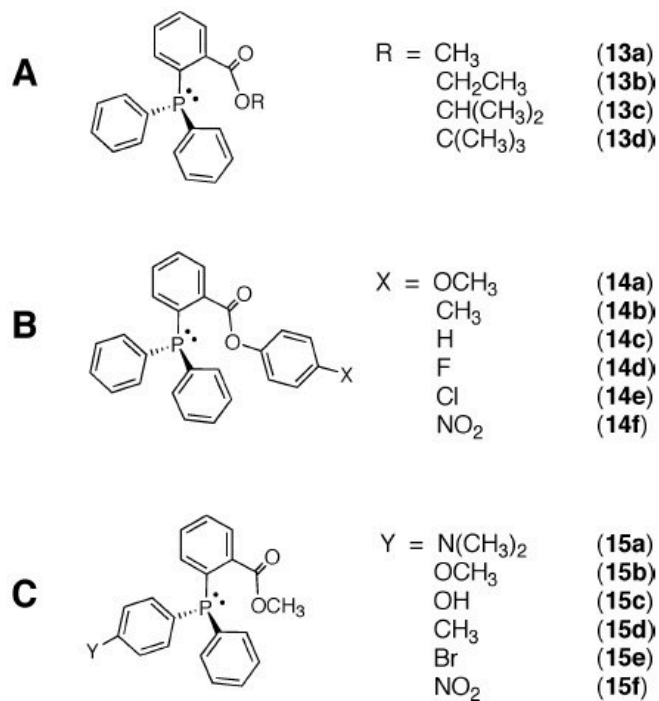
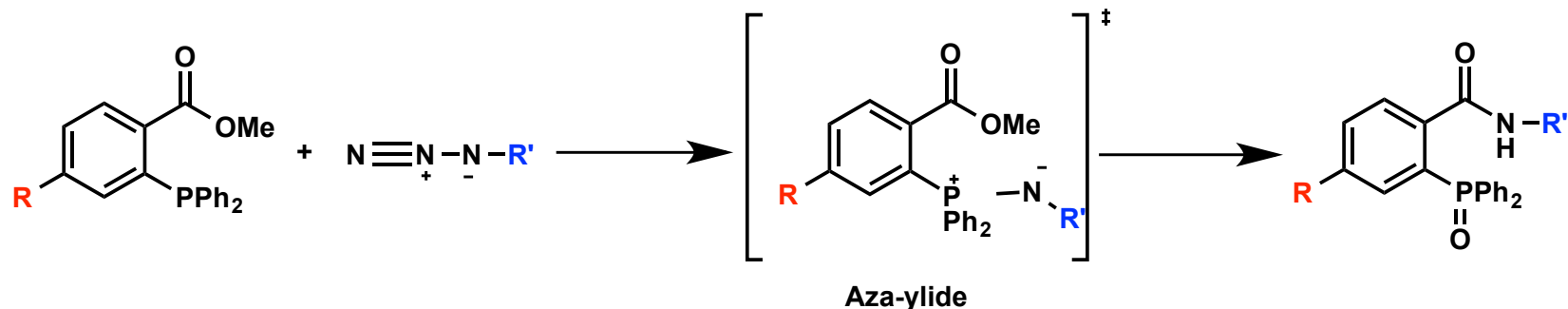


Figure 2. Phosphines synthesized to investigate the effects of steric and electronic modifications on the rate of the Staudinger ligation.

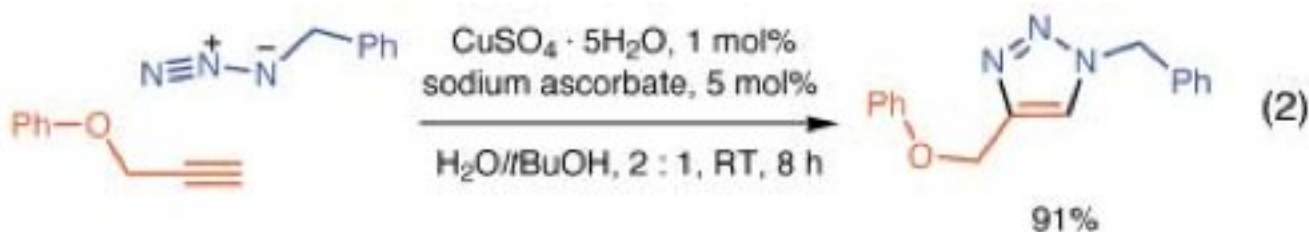
- Electron-donating groups on the phenyl group can accelerate the ligation.
- The leaving group doesn't affect kinetics though it determines the byproduct (primary amine) yield.

Brief summary of Staudinger ligation



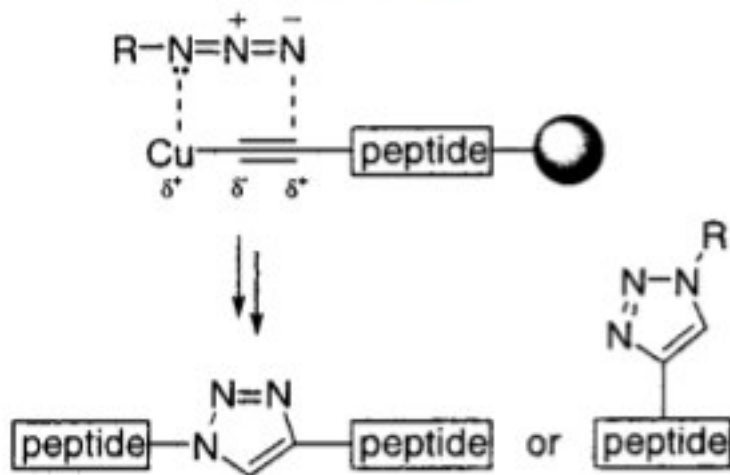
- The intramolecular reaction design enabled Staudinger ligation in water.
- Staudinger ligation accomplished labeling in cell lines and mice.
- Kinetics was not enough rapid to reduce the concentration of phosphine reagents though electron-donating group might improve it.

Second candidate – Click chemistry



Rostovtsev, V. V. ; Sharpless, K. B. *et al. Angew. Chem. Int. Ed.* **2002**, *41*, 2596.

Scheme 1. Copper(I)-Catalyzed 1,3-Dipolar Cycloaddition of Alkynes to Azides Affording Peptidotriazoles or *N*-Substituted Histidine Analogs



Tornøe, C. W. ; Christensen, C.; Meldal, M. *J. Org. Chem.* **2002**, *67*, 3057.

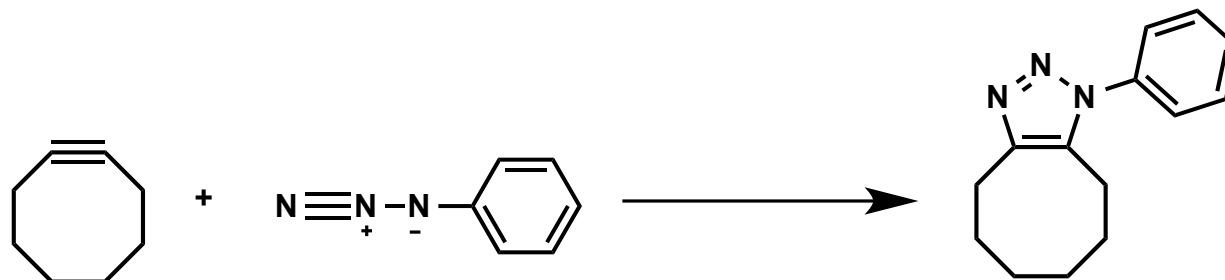
Cu(I) toxicity

✘ Detailed data was not published.

	Reagents	concentration	Survive time
Mammalian cells	Cu (I)	<500 μ M	1 h
Zebrafish embryo	CuSO ₄	1 mM	15 min
	Sodium ascorbate (Reductant)	1.5 mM	
	Tris(benzyltriazolylmethyl) amine ligand	0.1 mM	

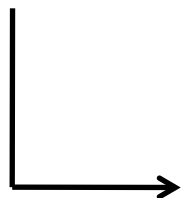
▪ Cu (I) showed high toxicity in the low concentration.
 → They intended to avoid using Cu.

Strain-promoted [3+2] cycloaddition

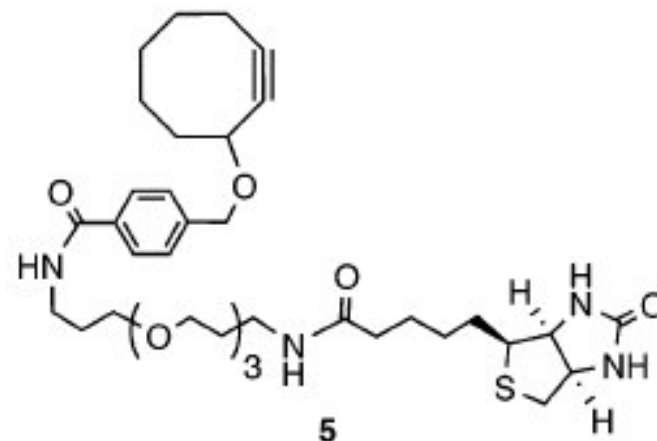


Wittig, G. ; Krebs, A. Chem. Ber. **1961**, 94, 3260.

Described as “*explosionsartig*”



Design of biotinylated cyclooctyne compound



Agard, N. J. ; Prescher, J. A. ; Bertozzi, C. R. *J. Am. Chem. Soc.* **2004**, 126, 15046.

Glycoprotein labeling

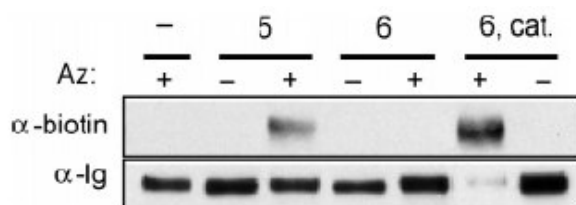
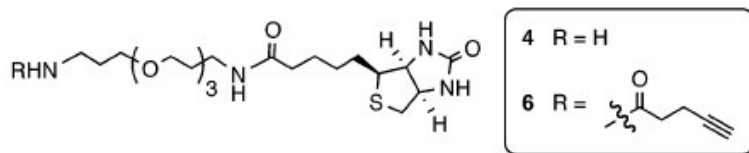
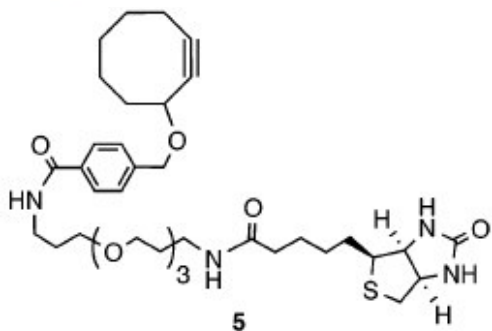


Figure 2. Labeling of azide-modified GlyCAM-Ig with alkyne probes. Purified GlyCAM-Ig was treated with buffer (–), 250 μM 5, or 250 μM 6 alone or in the presence (cat) of CuSO₄, TCEP, and a triazolyl ligand, overnight at room temperature. Reaction mixtures were quenched with 2-azidoethanol and analyzed by Western blot probing with HRP–α-biotin (upper panel). The blot was then stripped and reprobbed with HRP–α-Ig (lower panel).



3-2. Strain-promoted [3+2] cycloaddition Cell surface labeling

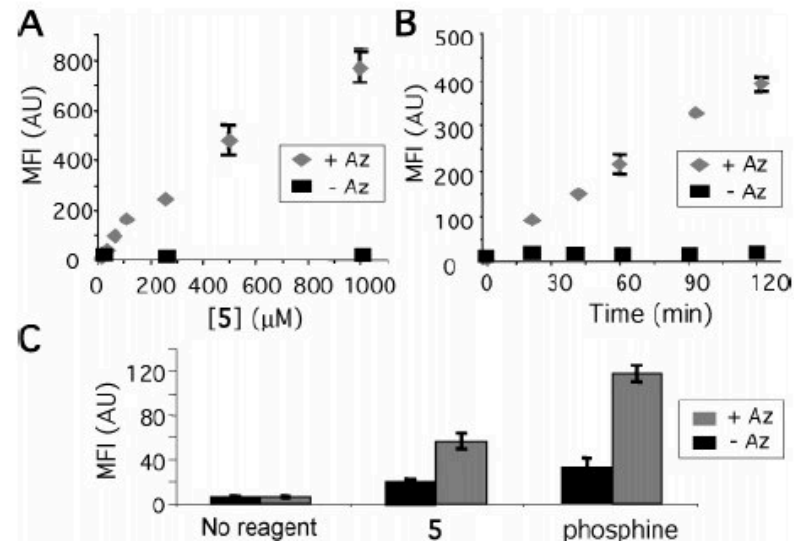
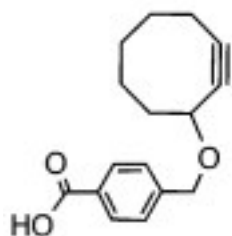


Figure 3. Cell-surface labeling with compound 5. Jurkat cells were incubated in the presence (+Az) or absence (–Az) of 25 μM Ac₄ManNAz for 3 d. (A) The cells were reacted with various concentrations of 5 for 1 h at room temperature and treated with FITC–avidin; mean fluorescence intensity (MFI) was determined by flow cytometry. (B) Cells were incubated with 250 μM 5 at room temperature and analyzed as in A. (C) Cells were incubated with 100 μM probe for 1 h at room temperature and analyzed as in A. Error bars represent the standard deviation from three replicates. AU = arbitrary fluorescence units.

- Application for covalent labeling of biomolecules and living cells succeeded.
- No apparent toxicity was exhibited.

Kinetics



OCT
 $k = 0.0024 \text{ M}^{-1} \text{ s}^{-1}$

Modification



3-2. Strain-promoted [3+2] cycloaddition

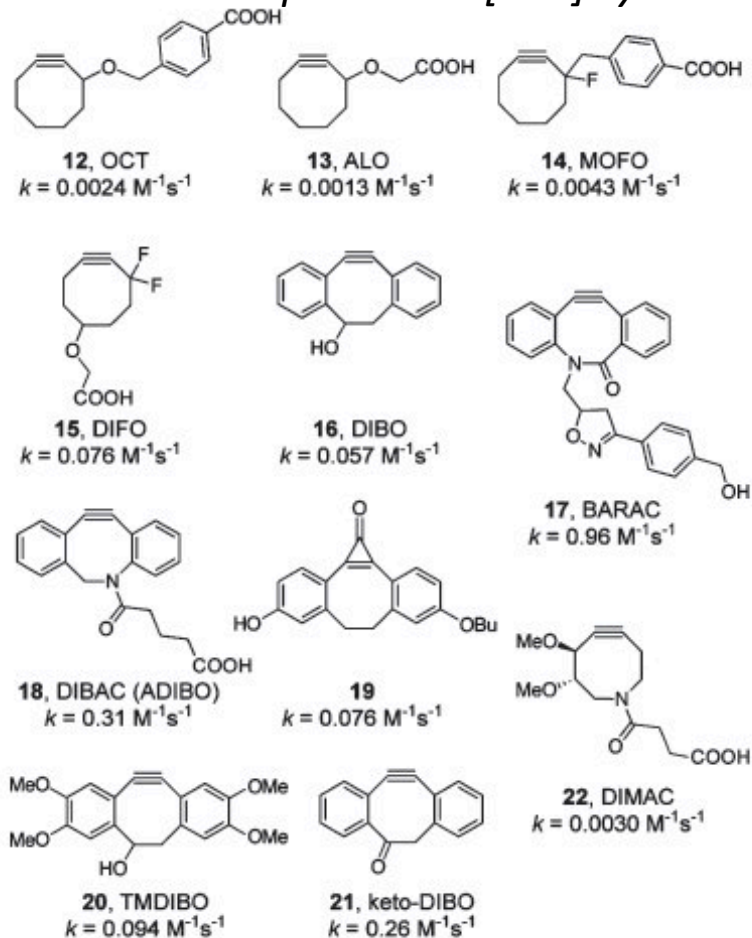


FIGURE 9. Cyclooctynes synthesized for Cu-free click chemistry in living systems. The second-order rate constants are for the reaction with benzyl azide in acetonitrile (**12**,²⁷ **13**,²⁸ **14**,²⁸ **15**,²⁹ **17**,³¹ **22**) or methanol (**16**,³⁶ **18**,³² **19**,³⁴ **20**,³⁵ **21**).

▪ The first Cu-free click chemistry reagent was only a little faster than Staudinger ligation.

→ Improvement was achieved by modification.

I'll take up DIFO and BARAC.

DIBO : Boons and co-workers
 DIBAC , 19: the Van Delft and Popik groups
 TMDIBO: Leeper and co-workers
 Others: Bertozzi group

DIFO : The reactivity is the same as Cu(I).

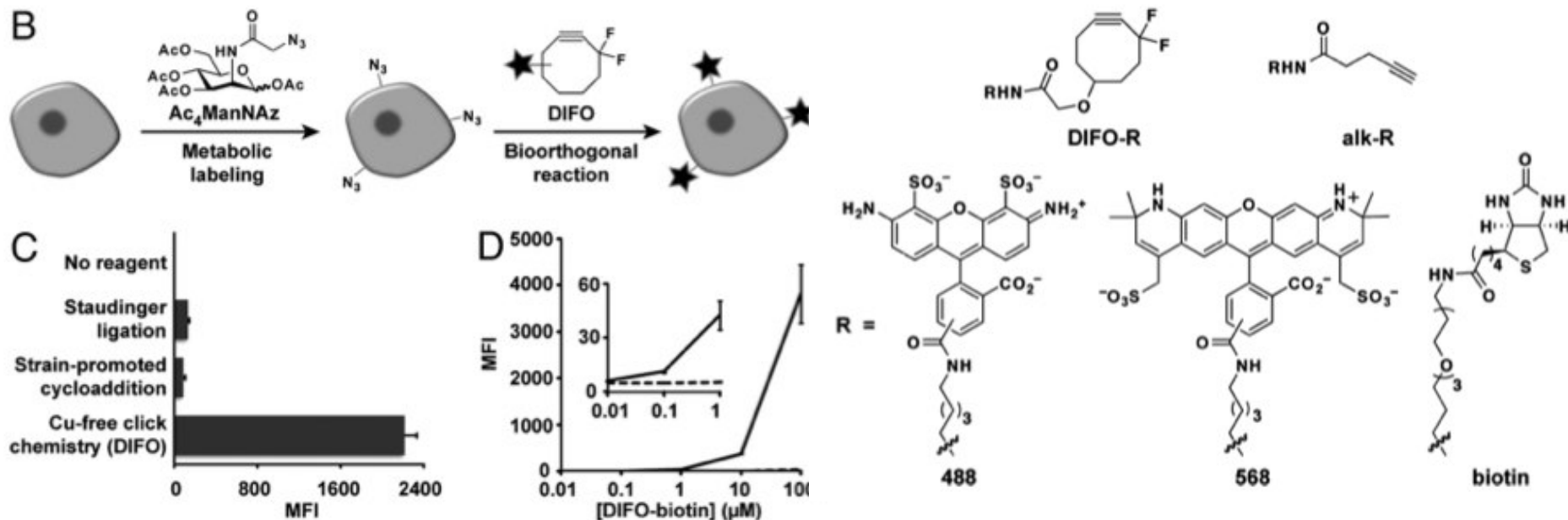
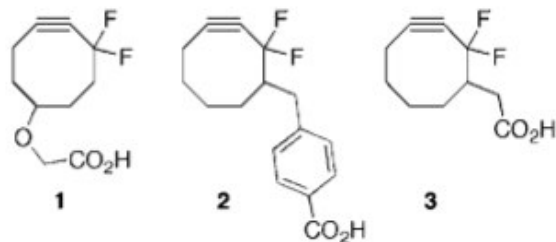


Fig. 2. Comparison of Cu-free click chemistry with existing bioorthogonal ligations. (A) Reactions of 10 ng of azidohomoalanine-labeled DHFR with 25 μM DIFO-488 or alk-488 were allowed to proceed for the time indicated. Reactions with alk-488 were performed as described in ref. 26. A negative control reaction (-) using 10 ng of azide-free DHFR was allowed to proceed for 60 min. (B) Schematic for metabolic labeling and detection of cell-surface glycans using Ac_4ManNAz and DIFO-based reagents. (C and D) Flow cytometry plots of labeling experiment described in B using Jurkat cells. (C) Cells were labeled for 1 h with 100 μM biotinylated derivatives of a phosphine (Staudinger ligation) (20), a nonfluorinated cyclooctyne (strain-promoted cycloaddition) (14), and DIFO (Cu-free click chemistry). In all cases, control cells (incubated in azido sugar-free medium but carried through an identical labeling procedure) displayed mean fluorescence intensity (MFI, arbitrary units) values <20 . (D) Cells were labeled for 1 h with 10 nM–100 μM DIFO-biotin. Error bars represent the standard deviation of three replicate experiments. Solid line, + Ac_4ManNAz ; dashed line, - Ac_4ManNAz .

▪ DIFO showed more rapid kinetics than the precedents and good reactivity in the low concentration.

Kinetics of DIFO



▪ Second-order rate constants of the reaction against benzyl azide.

cf) Staudinger ligation : $2.0 \times 10^{-3} \text{ M}^{-1} \text{ s}^{-1}$ (in CD_3CN)

	CD_3CN	7:3 $\text{CD}_3\text{CN} : 25\text{mM}$ potassium phosphate (D_2O , $\text{pH}=7$)
1	$7.6 \times 10^{-2} \text{ M}^{-1} \text{ s}^{-1}$	
2	$(4.2 \pm 0.1) \times 10^{-2} \text{ M}^{-1} \text{ s}^{-1}$	$(9.0 \pm 0.3) \times 10^{-2} \text{ M}^{-1} \text{ s}^{-1}$
3	$(5.2 \pm 0.2) \times 10^{-2} \text{ M}^{-1} \text{ s}^{-1}$	$(8.6 \pm 0.9) \times 10^{-2} \text{ M}^{-1} \text{ s}^{-1}$

Baskin, J. M. Bertozzi, C. R. *et al.* *Proc. Natl. Acad. Sci. U.S.A.* **2007**, *104*, 16793.

Codelli, J. A. Bertozzi, C. R. *et al.* *J. Am. Chem. Soc.* **2008**, *130*, 11486.

DIFO has realized live cell labeling.

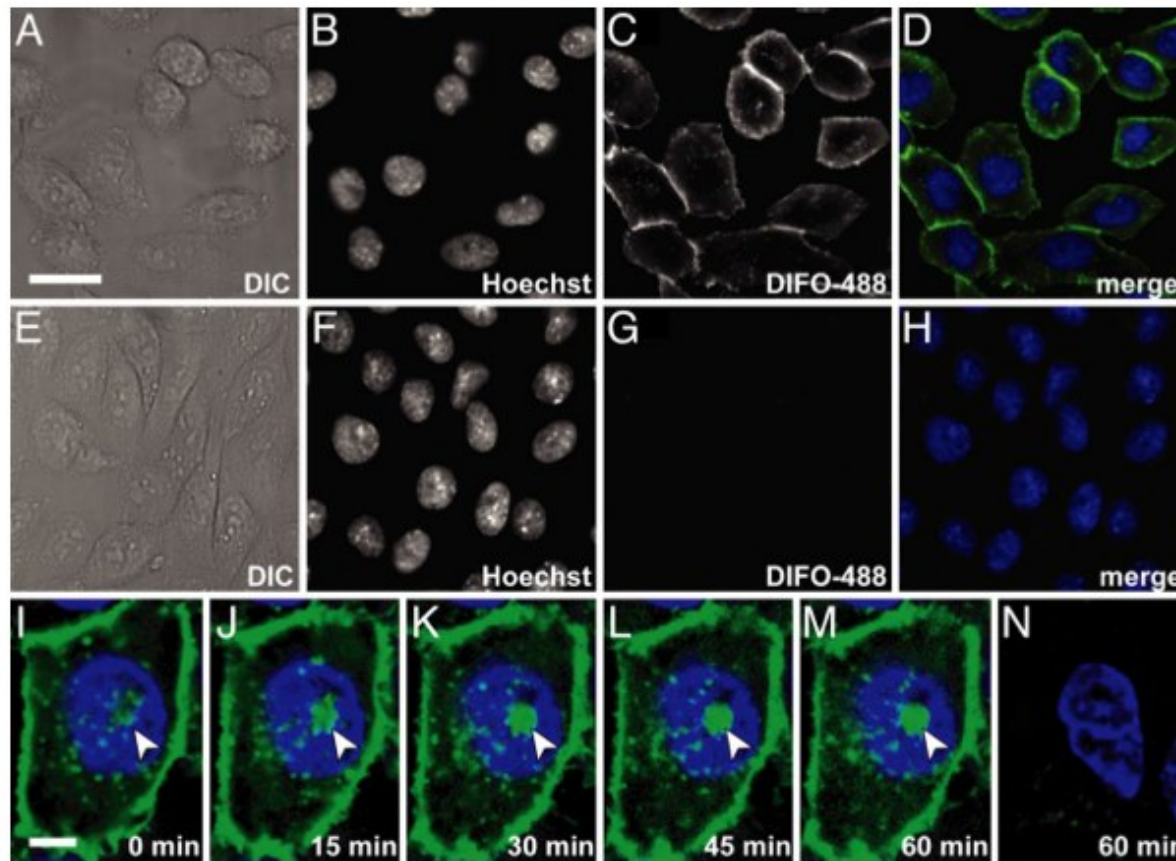
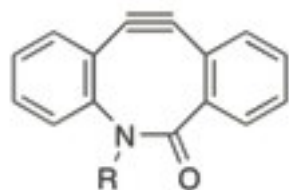


Fig. 3. Time-lapse imaging of glycan trafficking using an Alexa Fluor 488 derivative of DIFO. (A–H) CHO cells were incubated with 100 μ M Ac₄ManNAz (A–D) or 100 μ M Ac₄ManNAc as a negative control (E–H) for 3 days and subsequently labeled with 100 μ M DIFO-488 at 37°C for 1 min. (I–M) Time-lapse imaging of a single cell from the previous experiment over 1 h at 25°C (I–M, Ac₄ManNAz; N, Ac₄ManNAc).

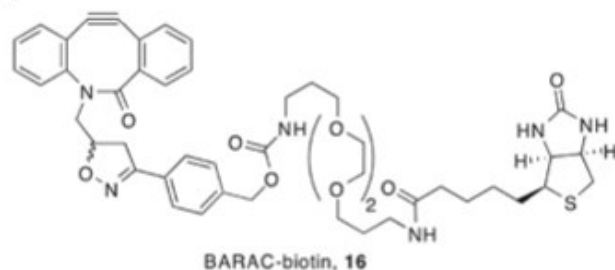
Superior to DIFO : BARAC



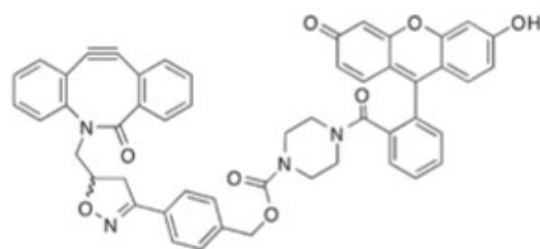
$$k = 0.96 \text{ M}^{-1} \text{ s}^{-1}$$

▪ BARAC was more reactive than DIFO.

1, BARAC



BARAC-biotin, 16



BARAC-Fluor, 17

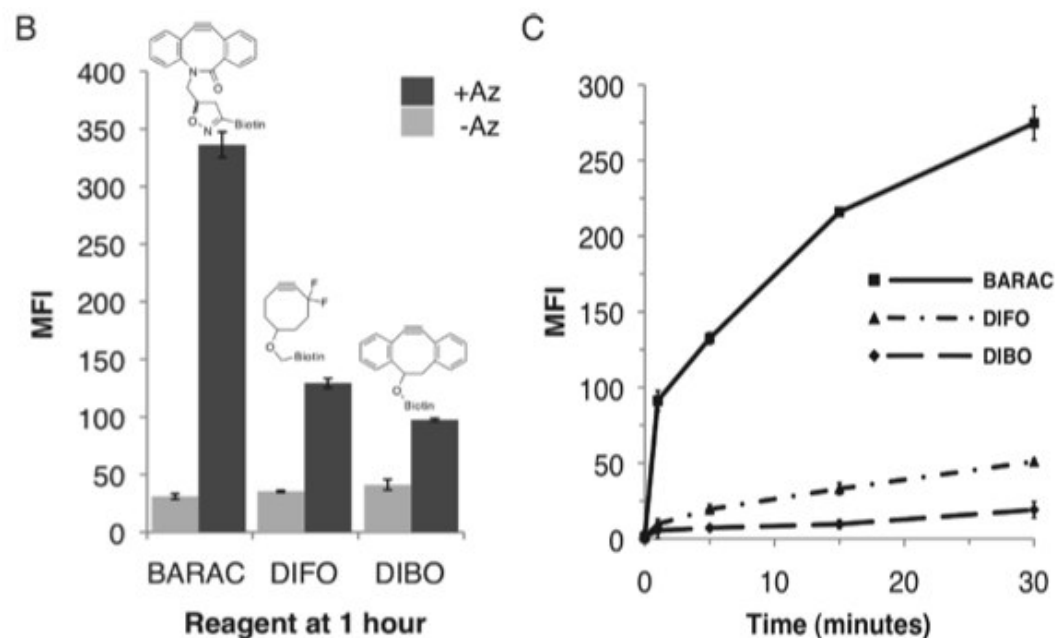


Figure 2. BARAC-probe conjugates label live cells with superior sensitivity compared to DIFO and DIBO reagents. (A) Structures of BARAC-biotin (**16**) and BARAC-Fluor (**17**). (B–C) Flow cytometry plots of live cell labeling with BARAC-biotin. Jurkat cells were incubated with (+Az) or without (–Az) 25 μM Ac_4ManNAz for 3 days. The cells were labeled with 1 μM cyclooctyne-biotin for various times and then treated with FITC-avidin. Cyclooctyne-biotin probes used were DIBO-biotin, BARAC-biotin, or DIFO-biotin. The degree of labeling was quantified by flow cytometry. The level of fluorescence is reported in mean fluorescence intensity (MFI, arbitrary unit). Error bars represent the standard deviation of three replicate experiments. (B) Comparison of the efficiencies of labeling of different cyclooctyne reagents after 1 h. (C) Time-dependent labeling of cyclooctyne-biotin probes. MFI reported as difference between signal of cells +Az and signal of cells –Az.

Washless labeling with BARAC

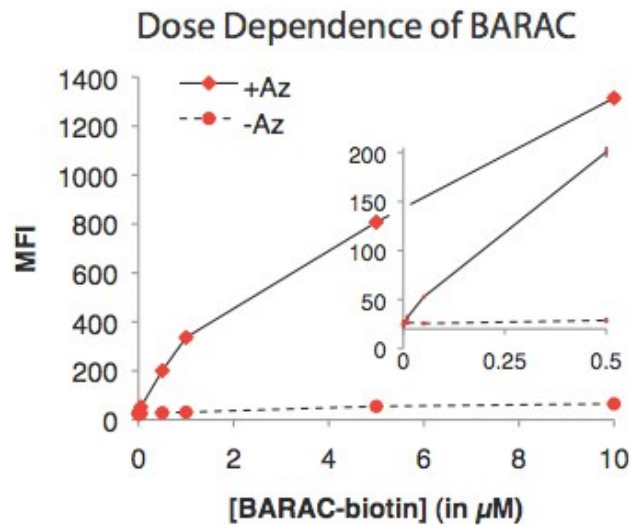


Figure S3. Cell-surface glycan labeling with BARAC-biotin conjugate **16**. Jurkat cells were incubated in the presence or absence of 25 μM Ac_4ManNAz for 3 d. Cells were reacted with no reagent (FACS buffer), BARAC-biotin conjugate **16** at varying concentrations in FACS buffer for 1 hour at 25 $^\circ\text{C}$, incubated with FITC-avidin, and analyzed by flow cytometry. The error bars represent standard deviations from three replicate samples (but are too small to see drawn to scale). MFI = mean fluorescence intensity and has arbitrary units (Au).

- BARAC's superior sensitivity allowed for use of *washless* labeling.
(rapid kinetics, low nonspecific background labeling)

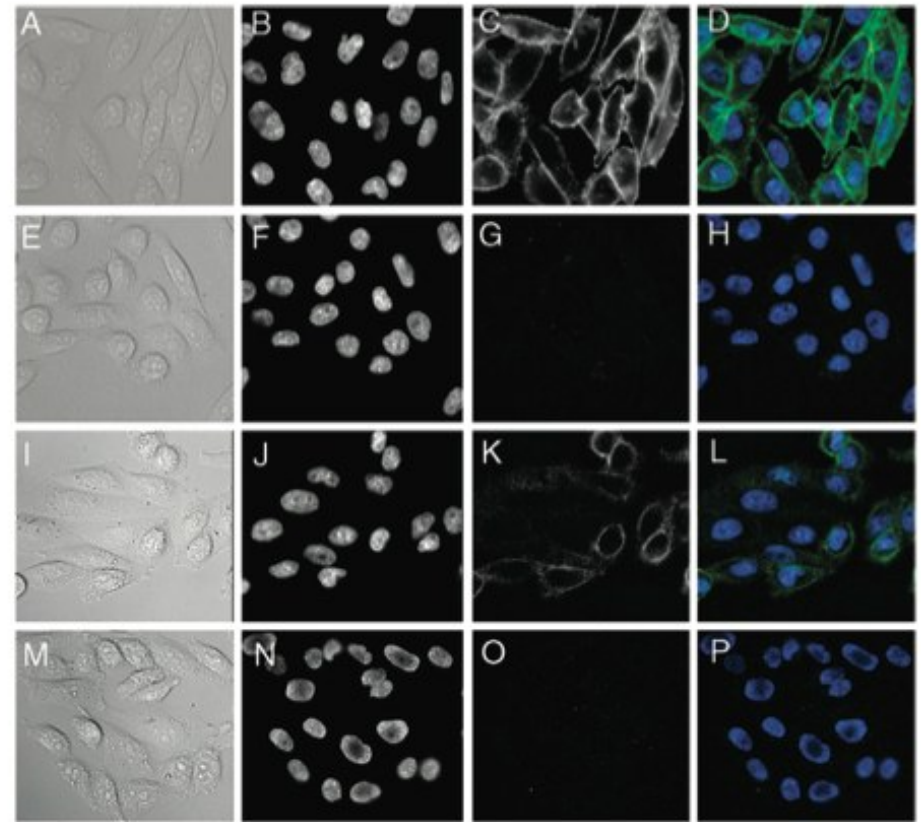


Figure 3. Imaging of azide-labeled glycans on live cells using BARAC-Fluor (**17**). (A–P) CHO cells were incubated with (A–D, I–L) or without (E–H, M–P) 50 μM Ac_4ManNAz for 3 days. (A–H) The cells were subsequently labeled with 5 μM BARAC-Fluor and Hoechst-33342 for 5 min and then washed and imaged. (I–P) The cells were subsequently labeled with 250 nM BARAC-Fluor for 30 min and Hoechst-33342 and then imaged without washing. Channels shown are differential interference contrast bright-field (A, E, I, M), the blue DAPI channel (B, F, J, N), the green FITC channel (C, G, K, O), and the DAPI/FITC channels merged (D, H, L, P).

Advanced labeling with DIFO *in vivo*

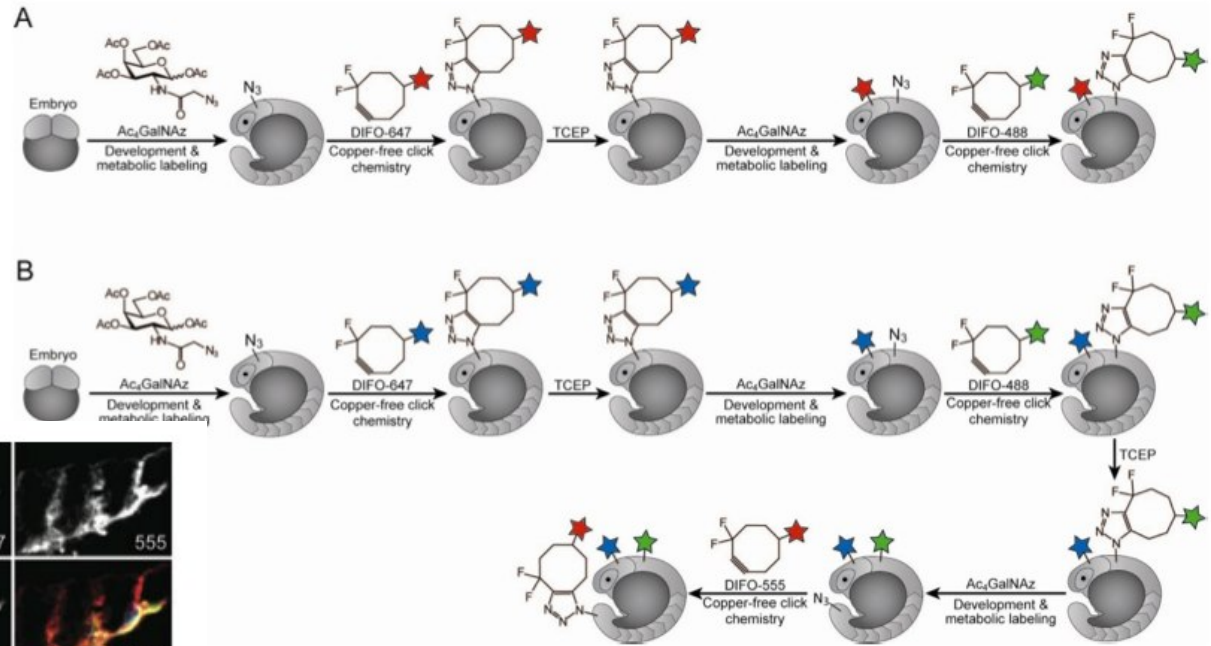
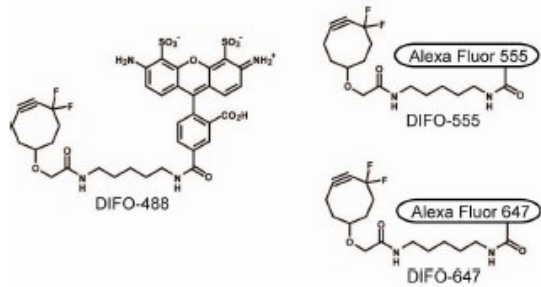
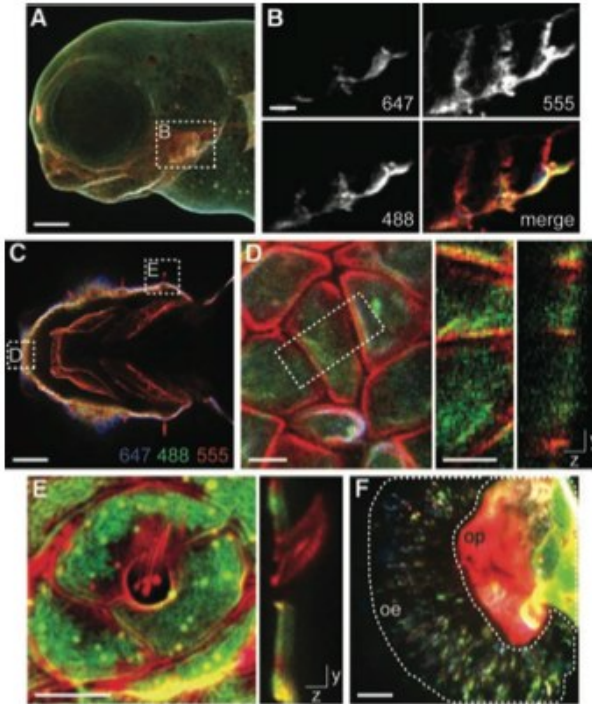


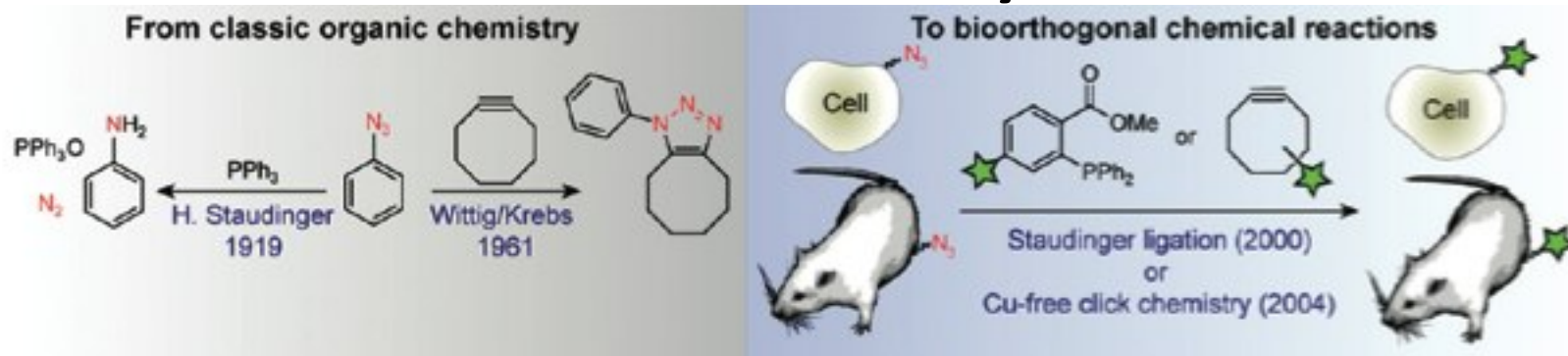
Fig. 4. Spatiotemporal analysis of de novo glycan biosynthesis during zebrafish development between 60 and 72 hpf. Zebrafish embryos metabolically labeled with $Ac_2GalNAz$ from 3 to 60 hpf were reacted with DIFO-647 between 60 and 61 hpf, metabolically labeled with $Ac_2GalNAz$ for 1 hour, and reacted with DIFO-488 between 62 and 63 hpf. The embryos were metabolically labeled with $Ac_2GalNAz$ for an additional 9 hours and then reacted with DIFO-555 between 72 and 73 hpf. (A) z-projection fluorescence image of a lateral view. (B) Single z-plane fluorescence images of the region highlighted in (A). (C) Single z-plane fluorescence image of a ventral view of the jaw region. (D) Left panel, z-projection fluorescence image of cells in the region highlighted in (C); middle and right panels, z-projection (middle panel) and x-projection (right panel) fluorescence images of the cells highlighted in the left panel (white dashed rectangle). (E) z-projection (left panel) and x-projection (right panel) fluorescence images of kinocilia. (F) z-projection fluorescence image of the olfactory organ. Highlighted are the olfactory epithelium (oe) and olfactory pit (op) regions. Blue, DIFO-647 (60 to 61 hpf); green, DIFO-488 (62 to 63 hpf); red, DIFO-555 (72 to 73 hpf). Scale bars in (A), and (C), 100 μm ; in (B), 25 μm ; in (D) and (F), 10 μm ; in (E), 5 μm .



- High reactive cyclooctyne DIFO realized multi-color imaging of the zebrafish embryo growth between 60 and 72 hpf. (hpf = hours post fertilization)

Laughlin, S. T. ; Bertozzi, C. R. et al. *Science* **2008**, 320, 664.

Summary



- Staudinger ligation and Strain-promoted click chemistry are highly applicable bioorthogonal reactions.
- In my opinion, the process of developing these reactions is full of suggestions for those who are interested in bio-applicable reactions.

Thank you for your kind attention.

Appendix

- Synthesis of biotinylated phosphine

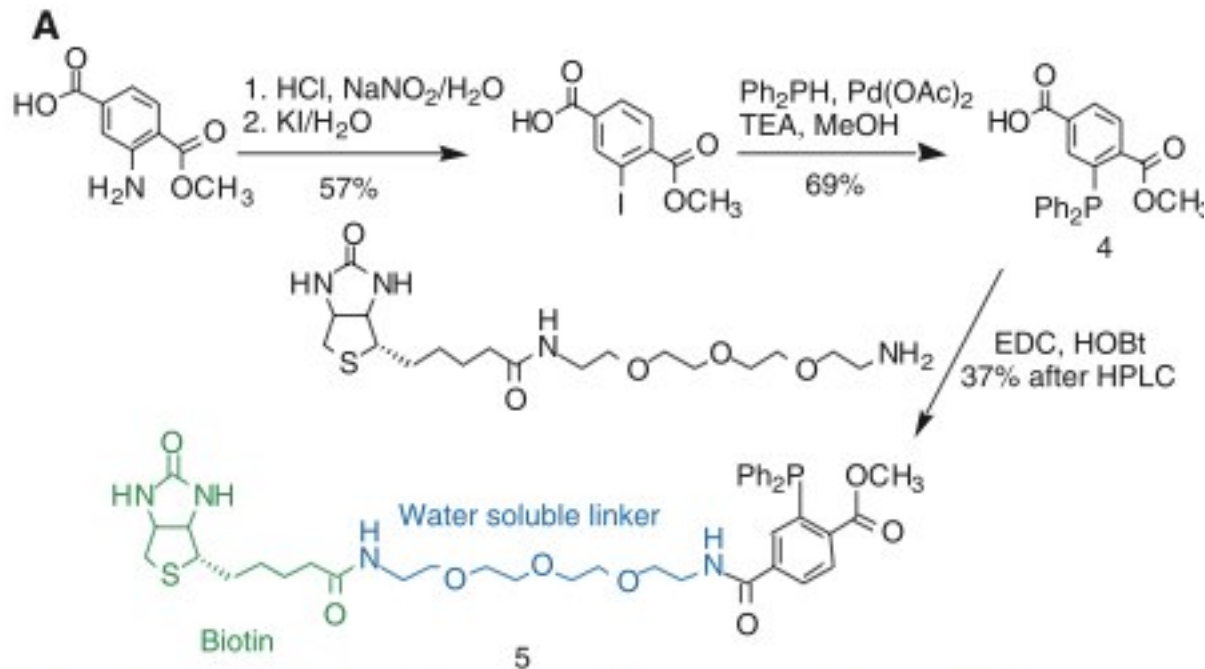
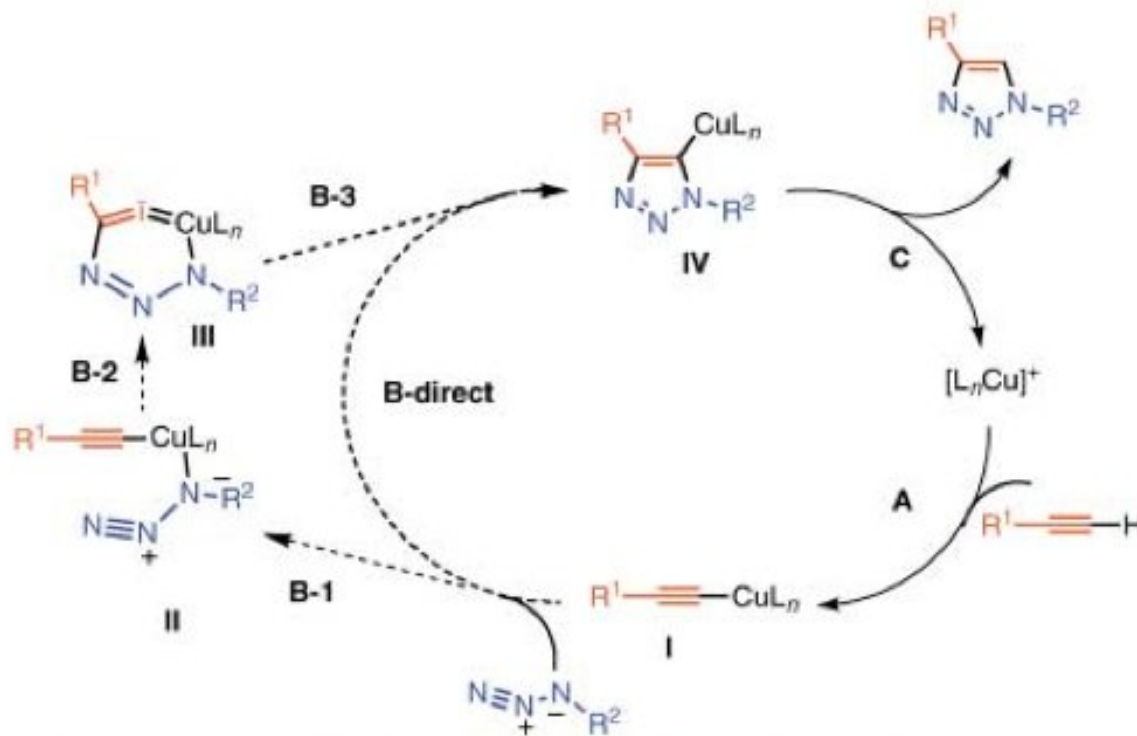


Fig. 3. Reaction of phosphines and azides on cell surfaces. **(A)** Synthesis of a water-soluble biotinylated phosphine for quantifying the reaction with cell surface azides [synthetic procedures for compound **4** are provided in (10)].

Mechanism of Cu (I) catalyzed click chemistry



Scheme 1. Proposed catalytic cycle for the Cu^I-catalyzed ligation.

Rostovtsev, V. V. ; Sharpless, K. B. *et al. Angew. Chem. Int. Ed.* **2002**, *41*, 2596.

Metabolic labeling of cell-surface glycans with Ac_4GalNAz

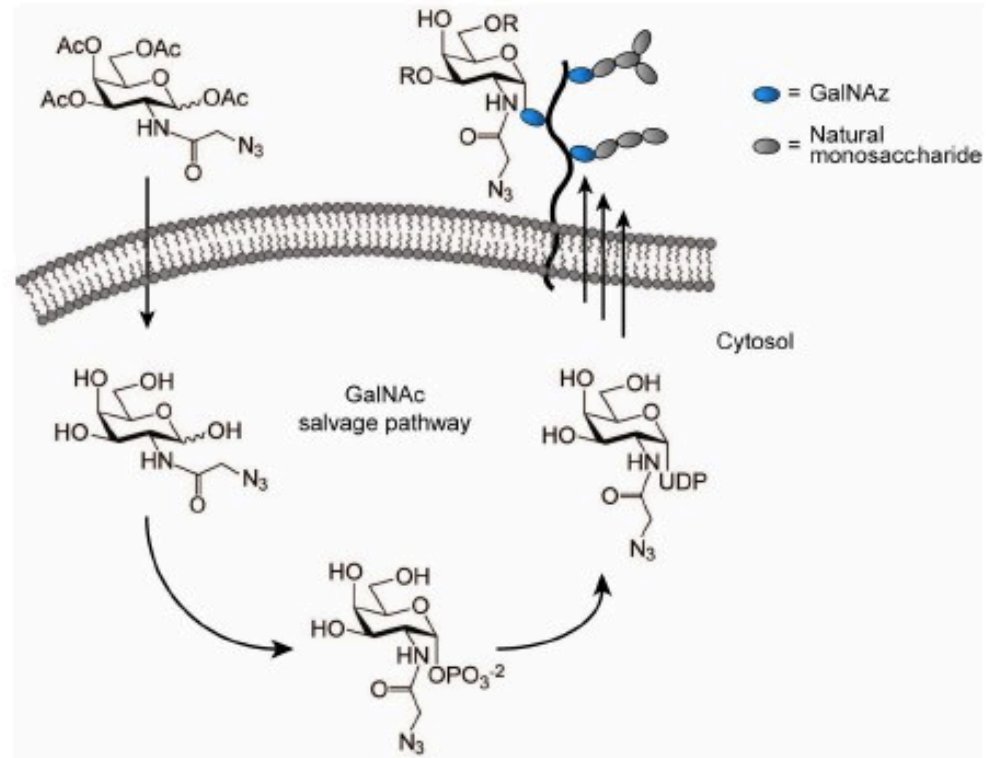


Figure S1. Strategy for the metabolic labeling of cell-surface glycans with Ac_4GalNAz . Ac_4GalNAz passively diffuses across the plasma membrane, is deacetylated by cytosolic esterases, and enters the GalNAc salvage pathway, where it is metabolically converted to the corresponding activated nucleotidyl sugar (UDP-GalNAz). UDP-GalNAz is in turn transported into the Golgi apparatus and appended to glycoconjugates by a family of glycosyltransferases. The resulting azido glycoconjugates are then trafficked to the cell surface. Ac, acetyl; R, additional sugar residues. Laughlin, S. T. ; Bertozzi, C. R. et al. *Science* **2008**, 320, 664.

The transition structure energy of DIFO is the lower than OCT.

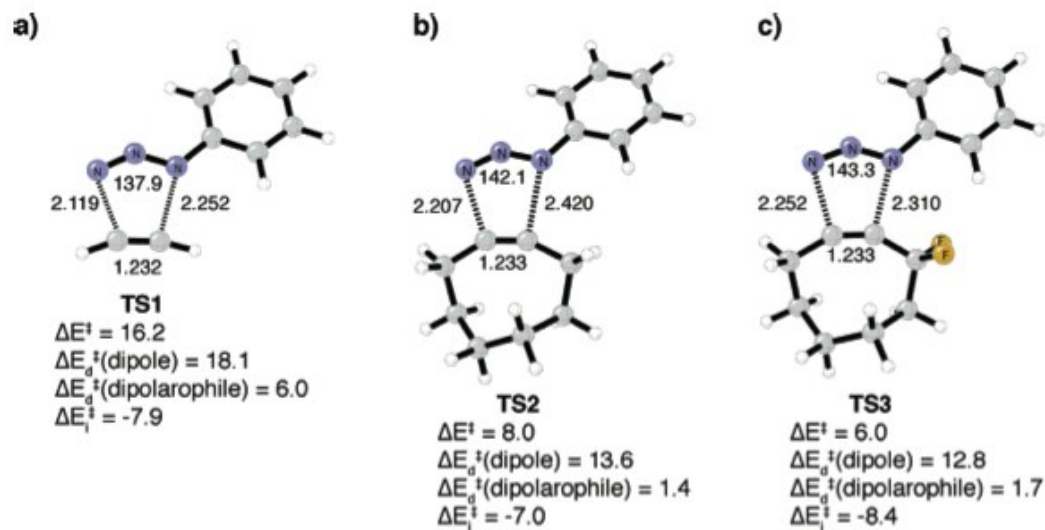
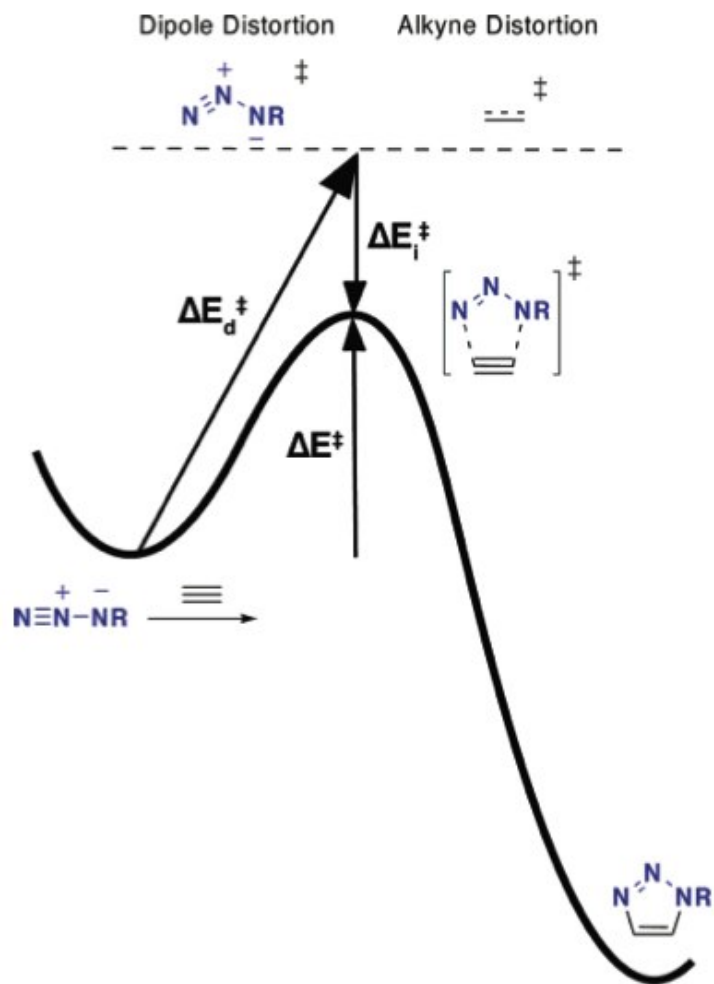


Figure 3. B3LYP/6-31G(d) ΔE^\ddagger , $\Delta E_d^\ddagger(\text{dipole})$, $\Delta E_d^\ddagger(\text{alkyne})$, and ΔE_i^\ddagger for the concerted transition structures of phenyl azide cycloaddition with (a) acetylene, (b) cyclooctyne, and (c) difluorocyclooctyne (kcal/mol). TS3 is the lowest energy regioisomer; see the Supporting Information.

Ess, D. H. ; Jones, G. O. ; Houk, K. N. *Org. Lett.*, **2008**, *10*, 1633.

Figure 2. Relationship between activation, distortion, and interaction energies for cycloaddition of an azide with an alkyne.

The reactivity enhancement of DIFO is caused by higher HOMO and lower LUMO.

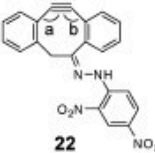
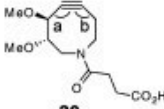
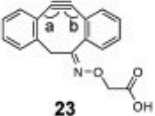
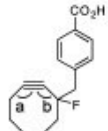
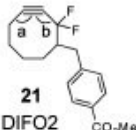
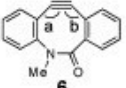
Orbtial Energies (au)

	HOMO	LUMO
Acetylene ground state	-0.41032	0.04195
Acetylene in TS1	-0.40439	0.04387
Cyclooctyne	-0.35118	0.04104
Cyclooctyne in TS2	-0.34877	0.04064
Acetylene in Cyclooctyne ground state geometry	-0.40772	0.04498
Distorted Acetylene in TS2 geometry	-0.4035	0.04492
3,3-Difluorocyclooctyne	-0.38726	0.03445

Ess, D. H. ; Jones, G. O. ; Houk, K. N. *Org. Lett.*, **2008**, *10*, 1633.

BARAC's high reactivity is due to the alkyne bond angle.

Table 1. Reactivity and Alkyne Bond Angles^a

cyclooctyne	a (°)	b (°)	rate constant (M ⁻¹ s ⁻¹)	ref.	cyclooctyne	a (°)	b (°)	rate constant (M ⁻¹ s ⁻¹)	ref.
 19 cyclooctyne	159	N/A	N/A	14	 22	152	157	N/A	18
 20 DIMAC	158	157	3.0 x 10 ⁻³	15, SI	 23	N/A	N/A	6.1 x 10 ^{-2**}	7b
 2 MOFO	160	155	4.3 x 10 ⁻³	6, SI	 24	156	155	6.3 x 10 ^{-2**}	14, 19
 21 DIFO2	162	151	4.2 x 10 ^{-2*}	17, SI	 6 BARAC	153	153	9 x 10 ⁻¹	7d, SI

^aCyclooctyne bond angles and second-order rate constants for the reaction with benzyl azide in acetonitrile at rt. All bond angles were measured via X-ray crystallography with the exception of compound 19, which was analyzed by electron diffraction in the gas phase. All data are referenced in the table, and details of the measurements first reported in this publication are located in the SI. N/A = data not available. *Rate was measured for the acid form of DIFO2. **Rate constant measured in methanol.

